Statistical mechanical model in legislative networks

Thesis submitted to Universidad de Chile

in partial fulfillment of the requirements for the degree of

Master in science with mention in Physics

Faculty of Sciences

by

Benjamín Edwards

March 9, 2024

Thesis Advisors: **Dr. Denisse Pastén**
Dr. Víctor Muñoz

FACULTY OF SCIENCES
UNIVERSIDAD DE CHILE

APPROVAL REPORT
MASTER THESIS

The Graduate School of the Faculty of Sciences is informed that the Master's Thesis presented by the candidate

Benjamín Edwards

has been approved by the Thesis Evaluation Committee as a requirement for the Master's degree, in the Private Thesis Defense examination given on YYYY-MM-DD.

Thesis Advisors

Dr. Denisse Pastén _____

Dr. Víctor Muñoz _____

Thesis Evaluation Committee

Dr. Sergio Davis _____

Dr. Flavia Pennini _____

Optional dedication.

Biography

Benjamín Matías Edwards Ortiz was born in Rancagua, Chile on February 10, 1997. He is the son of Javiera, the big brother of Jacinta, and the eldest grandson of Lupe and Gustavo. Since he was a child he developed an ease with mathematics and always were curious about how things work. In an attempt of answer his questions about the world, his grandparent Gustavo gave him explanations based on Physics, feeding his desire to know more and more.

In high school Mathematics and Physics were his favorite courses and wondered if he should purse an Engineering or Physics career. Looking to make up his mind, on 2014's summer, with the support of his family, he took a Physics course on Universidad de Chile's Summer School and a year later joined Universidad de Chile's Faculty of Sciences to study his Physics degree where he confirmed his academic interests.

On 2021 he began his Master in Physics at the same house of studies, process that culminates with the presentation of this thesis.

Acknoledgements

I would like to thank my advisors Denisse and Víctor for give me a space were I could mix physics with social and political studies. Also, I thank my family and friends, who have supported me through this process.

This thesis and was funded by ANID Chile through FONDECYT grant N° 1201967 (Principal Investigator: Dr. Víctor Muñoz).

Abstract

Looking for ways to quantify political polarization on parliaments, we have built a statistical mechanics model for the specific case of a legislative networks from roll-call votes. For this we have considered a network of legislators that is fully connected and whose links have assigned values of 1 or -1 accordingly if a pair representatives have vote the same or not. Then, we have taken links a triangles in the networks as spins, and from there we developed a mathematical formalism which led us to derive expression for magnetizations, entropies, energy and temperature for the system.

Resumen

En busca de cuantificar la polarización política en parlamentos, hemos construido un modelo de mecánica estadística para el caso específico de una red legislativa creada a partir de votos en sala. Para esto hemos considerado una red the parlamentarios completamente conectada, a cuyas conexiones se les han asignado los valores de 1 o -1 según cada par de parlamentarios votó lo mismo o no. Luego, he considerado las conexiones y triángulos presentes en la red como espines, y a partir de esto hemos elaborado un formalismo matemático que nos condujo a obtener expresiones para magnetizaciones, entropies, energía y temperatura del sistema.

Contents

Biography **iii**

Acknoledgements **iv**

Abstract **v**

Resumen **v**

1 Introduction **5**

1.1 Statistical mechanics of social systems 5

1.2 Graph theory and complex networks 7

1.3 Legislative networks 9

1.3.1 Polarization in legislative networks 12

2 Model **15**

2.1 The configuration space 16

2.2 Spins system 17

2.3 Counting links and triangles 17

2.3.1 Links 19

2.3.2 Triangles 20

2.4 Magnetizations and energy 26

2.4.1 Magnetization 26

2.4.2 Hamiltonian 27
2.4.3 Alternative form for the energy 29
2.5 Entropies 31
2.5.1 Using Boltzmann entropy 31
2.5.2 Using Shannon entropy 32
2.5.3 Entropy in terms of magnetization 33
2.6 Temperature 35
2.6.1 Additional relations with temperature 36

3 Model analysis **39**
3.1 Configuration space for $k = 3$ and $N = 155$ 39
3.2 Magnetizations and entropies 40
3.2.1 Minimum of m_ℓ and maximum of s_ℓ 44
3.2.2 Relationship between magnetizations and entropies 51
3.2.3 Relation between m_ℓ and m_t 53
3.3 Temperature 58
3.3.1 Looking the analytical expressions 59
3.3.2 Temperature in the configuration space 60

4 Evaluation of the model with data **65**
4.1 About the Chilean Chamber of Deputies 65
4.2 Gathering data 66
4.3 Vote records analysis 67

5 Discussion and conclusions **73**
5.1 About related work 73
5.2 About strong polarization 75
5.3 About the physical magnitudes 76

5.3.1 Magnetizations and energy 76
5.3.2 Entropies 77
5.3.3 Temperature 78
5.4 Final conclusions 78

Bibliography **81**

Chapter 1

Introduction

As the lector may expect given the title, this thesis is about an statistical mechanical model on the legislative process, for the sake of redundancy, on legislative institutions or parliaments. Specifically, the work present in the following chapters addresses the vote process and how the legislators can agree or disagree between themselves on it. Given that, assuming the lector might come from a physics background, in the rest of this chapter I am going to give some context about how we ended up studying topics that are often seen very far from theoretical physics, with physics tools. I am also going to introduce fundamental topics for this work. Specifically, about graph theory and complex networks, about using signed links on them, and about similar studies that have analysed relations inside legislative institutions that motivated this work.

1.1 Statistical mechanics of social systems

In the last decades there has been an increasing trend to tackle social phenomena with statistical physics, usually, taking social interactions as interactions between agents that may have different states [1]. The states may be political opinions, cultural or

linguistic traits, for example. Some examples are works on opinion dynamics [2–8], cultural dissemination [9, 10], language dynamics [10, 11].

Although, despite these works may model different social phenomena, if we simplify the majority of them for a moment, we can summarize them all by saying in these models the agents interact between themselves —assuming that these interaction mean some sort of opinion, cultural or language exchange— and update their states according to some predefined rules, iteratively. That way, usually, the systems evolve to whether an ordered or unordered situation, with order representing consensus, agreement, or uniformity, while disorder standing for fragmentation or disagreement [1].

These processes actually occur on real social systems. Social sciences have already studied it, having, for example, scholars from those areas naming "social pressure" [12] to the phenomena that would explain why interacting people become more alike. And with the same purpose, from physics we can also came up with analogies, like ferromagnetic interaction on magnets for agents becoming more similar if they interact, and anti-ferromagnetic for agents becoming more different.

Given this background, we are encouraged to keep employing statistical mechanics tools for this purpose. In our case, while our subject of study are the legislators and how the vote, we clarify that our approach is different from the mentioned examples. The model we propose is not going to be about simulations of how a parliament would evolve from vote to vote. But, it is going to be about the statistics of all possible interactions between legislators given a particular vote. If wanted, it is going to be a micro-canonical formalism rather than a canonical one.

1.2 Graph theory and complex networks

Graph theory is a fundamental area of mathematics and computer science that has found applications in various disciplines. It deals with the study of graphs, which are mathematical structures used to model pairwise relations between objects through nodes connected with links, which can also have a defined orientations, with a source and a destination node.

It started on 1741 with Euler's work on the problem known as "Seven Bridges of Königsberg", which consisted on determine a path to walk over the city crossing seven bridges that connected the two mainlands and two islands, without passing more than once through each bridge. Euler treated each patch of land as different nodes connected with links that represented the bridges, and analyzing the resulting graph he proved —mathematically— that there was no possible path for that task (and constraints) [13]. Nowadays the relevance of graph theory extends beyond mathematics, having found applications in diverse fields such as neuroscience [14], ecology [15], epidemiology [16], psychology [17, 18], geography [19, 20], and studying real-life and online social networks [21, 22], for instance.

Complex network analysis, on the other hand, employs graph theory for representing real-world complex systems as complex networks. These are usually characterized by non-trivial topological features such as small-world properties [23], scale-free degree distributions [24], and community structures [25–27]. They have also been used in different areas, as the study of social networks [28, 29], networks on internet [28], biological networks [28, 30]; on epidemiology [31], more recently identifying spreader agents of COVID-19 [32]; and also on the categorization of magnetospheric storms [33], to mention a few examples.

The development of both graph theory and complex networks has been marked by the study of different subtopics as generative models, specially since the late 50's until the end of the millennia, and the development of different major techniques for community detection, since early 2000's until present day. On 1959 Erdős and Rényi proposed a model [34] for random graphs given raise to other studies on generative models decades later as, for example, the Watts-Strogatz model for small-world networks [23] and Barabási-Albert model for scale-free networks [24]. Later, despite there had been different tries on standardize how to detect communities on networks by the end of the 1900's, was not until 2004 a method started to be establish itself in the area. Concretely, Newman & Girvan [25] proposed modularity as a measure for quantifying how much fragmented a network was, and stated the best partition of communities was the one that maximises modularity. They proposed an algorithm for this task, but in the following years plenty of works dedicated to address modularity maximization as a goal, looking for improving and optimize the process —due the NP complexity of the problem itself. A few of them are Clauset *et al.* [35], Duch & Arenas [36], and Blondel *et al.* [37]. At that time Reichardt & Bornholdt [38] proposed an algorithm for detect communities based on statistical mechanics. They proposed a hamiltonian whose minimization conducted to the best community partition and also they proved that under some consideration for some parameters fo the model, that minimization was equivalent to modularity maximization. Finally, since early 2010's until present day we can see how Stochastic Block Model [39–41] has been taking its place among community detection paradigms, employing Bayesian inference and establishing itself as the go-to way to infer communities or "block" structures from connections.

Although they are related, graph theory and complex networks analysis (CNA) are not necessarily the same. We are going to refer as graph theory to the analysis

of more geometrical and topological properties of small graphs, while as complex network to the modeling of real systems with networks or graphs with high number of nodes and/or links, often involving the analysis of real data. If wanted, graph theory may lean to be more theoretical and abstract, while CNA to be much more specific and concrete, regarding the studied system.

Finally, we say in advance the work in this thesis is in between these two already-related topics. The motivation for our work comes from the branch of complex networks dedicated to legislative network (more about this on Section 1.3), but the theoretical development we propose in Chapter 2 is going to be closer to graph theory. However, in Chapter 4 we will briefly analyze a real-world dataset of vote records.

1.3 Legislative networks

An area where without a doubt complex networks have had great impact, are social sciences —sociology, anthropology or behaviour science and psychology, to mention a few. Networks allow us to study relations between people (or groups of people) as connections between nodes. This is easy to see on online social networks, where there are explicit interaction users may have. Follows, likes, mentions and replies are, for instance, social interactions nowadays are common to be seen on the online world. But, letting the internet apart, real world social interaction can also be taken into account. Friendship, partnership, sexual relations, work relations, and even political relations can be subject of study [42].

A particular social relation is the political relation legislators may have between each other due the legislative process. This relation is indeed one of the main cornerstones of this thesis since our subject of study are posible underlying relation between parliamentarians as result of their behaviour while voting. Works that address this

relations with a network approach are often called to be about "legislative network" in the literature. So, in this section we give the lector some background about this topic.

As context, most works on legislative networks [43–56] are characterized by analyze underlying interaction or relations between legislators to get a picture of non-explicit alliances or fractures in the legislative process. Means relationships between parliamentarians are inferred from vary from work to work. Most commons are bill co-sponsorship [43, 50, 54, 55], co-assistance to legislative committees or press events [51], and coordination on roll-call votes [44–46, 52, 57].

Usually, the network construction is followed with community detection and a comparison between the resulted partition with the partition derived from political parties. Also, many works look up for ways to quantify political polarization, commonly, evaluating how much "polarized" is the community partition resulted from the community detection process with different metrics —such as modularity [26, 27, 43].

In this thesis we opted by model a network constructed from the agreement parliamentarians may have when they vote. But, how do we map a vote into a network? We found that even within the subgroup of legislative network studies that consider roll-call votes as a mean to relate legislators from, there is no unique way to do it. Different works connect the legislators in different ways, since each work may have different goals.

For instance, Waugh *et al.* [57] connected a pair of legislators if they voted the same, and if they did not, simply there is no link between them. But, in order to study the polarization in the U.S. Congress through the years (decades, actually), the authors actually consider roll-call data from an entire legislatures to build a single network. Their work's methodology consists on build a sequence of networks

whose polarization can be measure to obtain a polarization time-series later. Each network is made from all votes made on a two-year span of legislative activity. So, actually, since they consider multiple votes to build one network, they put the number of votes in which a pair of parliamentarians have agreed as the weight of the link between each pair of representatives. On the other side, other works have proposed more elaborated process from which infer relations between members of parliaments (MP). Andris *et al.* [52] also studied the U.S. Congress taking each legislature as a network, but they built the networks differently. For each legislative term they estimate a threshold of amount of coordinated votes a pair of parliamentarians must surpass in order to be taken as connected. Marenco *et al.* [44] used roll-call votes of the Brazilian Chamber of Deputies for a period running from 2003 to 2018. Authors assign different scores to each vote options and build yearly sequences of roll-call options scores, for each MP. Later, they build up a correlation distance from those sequences which is taken as the links distance. Finally, Intal & Yasseri [45] analyzed the 57th UK Parliament and focused principally on Brexit discussions. For each MP, the authors built a sequence of their votes with its entries 1 or -1 if they voted for or against. Then, they computed the cosine similarity between every legislator votes sequences, which was later used to derived the links between parliamentarians, and their respective weights.

In this work, in contrast to these works, we will limit ourselves to analyze (theoretically) one single vote rather than taking multiple ones into account. As we will see later we will connect all legislators between each other, and the links between them are going to get values of 1 or -1 assigned accordingly if the vote options for each pair matched or not. This sign assignment to the links has been inspired by [43], work that will be discussed below.

Polarization in legislative networks

In order to study how polarized a legislative network is, detecting communities on it is needed. Commonly *polarization* is referred when the network has two main communities, while if there are more that two relevant communities is often called *fragmentation*. Now, leaving that semantic distinction aside and sticking with *polarization*, it is considered that legislative networks are polarized when legislators that belong to the same community have stronger interaction within themselves, while weaker (or non existent) with legislators of different communities. Neal [43] take this conception of polarization as *weak polarization* an then proceeds to defined *strong polarization*. This one, in addition to taking into account intense links between nodes from the same group, is characterized by considering that nodes from different communities should also have links that join them, but this time with weights whose signs will be negative. A possible way to think of this is to take positive sign links as attractive forces, while negative counterparts as repulsive ones. All this is only applicable in a network that have signed links. For this, the author uses a data set of bills co-sponsorship and employs the Stochastic Degree Sequence Model algorithm [58] on it to infer the positive and negative links. Instead, we will not consider co-sponsorship relations but vote options agreements. More details on how we will construct the network in our model will be on Chapter 2.

Regarding the quantification of *strong polarization*, instead of using modularity as a proxy for it —since the network have links with negative values—, in [43] the author propose the triangle-index for that purpose [59]. This metric comes from balance theory, and it tells how much *balanced* the network is. Now, what does it mean by *balanced*? For this we are going to introduce what is balance theory, briefly.

Balance theory established in psychology as itself with the Cartwright & Harary

[60] formulation of Heider [61] theory. It started as way to characterize transitive relations between people or objects, but the most common example to understand the idea behind "balance" comes from considering a system of three people: If all of them are getting along there is no problem. But, if two of them get into a fight, probably each of them are going to ask the third to take side, and if the third does not want to, the system it is going to be unstable. In this context it is going to be called *unbalanced*. The balance —in this example— it would mean there is no pair of people that share how they feel about the third one. This triadic relationship can be mapped into a graph of three nodes connected with each other, and with links weight values equal to positive or negative whether the relationship are good or not, respectively. Then, a more concrete definition for balancedness in triangles will be to take the triangle as balanced if the product of the link signs is positive one, and as unbalanced otherwise.

At some point this also will be analogous to the frustration problem in a system constituted by three spins where there is at least one antiferromagnetic interaction. For that system will the minimum energy will be degenerated and the system itself will be prone to switch or cycle through different configurations with the same energy.

Starting from that notion with three nodes, balance theory then will also study the balance in bigger cycles. Different metrics have been developed to quantify balance [59, 62], but in this work we will limit ourselves to consider triadic relationships (or triangles) since they are the most basic cycle we can measure the balance of.

Chapter 2

Model

In this chapter we are going to explain the proposed model. Summarizing, it consists on statistical mechanical formalism for the specific case of agreement networks on parliaments. The model consider **a single vote session** in which each legislator chose one of k vote options. Usually, k is three since most common vote options are *for*, *against*, and *abstain*, but we developed the mathematical formalism for an arbitrary number of votes options.

The network consists on N nodes —each one representing on legislator— and they are all connected with each other. We assume parliamentarians develop likeliness toward others that vote the same and enmity to those who do it differently. Thus, the links between each pair have a weight or value equal to +1 if they voted the same and -1 otherwise. The statistical mechanics instead of being focused on the legislators it will be focused on pairs or triads of them. In other words, we are going to develop the physics for this network from its links and triangles.

2.1 The configuration space

We are interested on study all possible configurations the network could be in. We consider the nodes indistinguishable so we do not care of who voted this or that option, but how many parliamentarians voted for each one. In other terms, the amount of MP's that backed each vote option are our generalized variables, since knowing them we can completely describe our system. For now on we are going to denote a general configuration the network could be in as the vector $\vec{n} = (n_2, n_2, \ldots, n_k)$, with its entries n_i being the number of legislators (nodes) that chose the i-th vote option.

Noticing that the sum of all of its entries equals the total number of nodes legislators N, we get

$$n_1 + n_2 + \ldots + n_k = N. \tag{2.1}$$

which completely describes our configuration space. For lower, say $k = 2$, this space is going to be a straight line in a two-dimensional space, while for $k = 3$ it would describe a plane on a three-dimensional space. This last case can be plotted and will be presented on following chapters.

Hereinafter, we are going to refer to some specific vote scenarios or network configurations as follows.

- *Unanimity.* When a vote has all the votes, or in other words when for some vote option a, $n_a = N$ and $n_b = 0$ and $\forall\, b \neq a$.

- *Split in half.* When a vote is equally disputed between two options, which is equivalent to say when $n_a = n_b = \frac{N}{2}$ and $n_c = 0, \forall c \neq a \neq b$.

- *Center of the configuration space.* The scenario when $n_a = N/k, \forall a \in \{1, \ldots, k\}$. For the specific case of $k = 3$, will also be referred as *split in third*.

2.2 Spins system

Inspired in the Ising model we decided to also interpret own quantities from the network in a similar way as spins on the Ising model. We chose the links signs and triangles balances since these tell us the agreement between parliamentarians and if the triads are balanced or not. Also, both can only have values of +1 or -1, which coincides with the Ising framework.

It can be seen easily signed network can only have four types of possible different triangles. Two balanced $([+++], [+--])$ and two unbalanced $([---], [++-])$. Instead, in this model we are only going to have just three of them. By following the construction rule of the network we imposed (which consisted on assigning links values of +1 between legislators that voted the same, and -1 otherwise) it is impossible that triangles of type $[++-]$ appear, leaving us with two balanced and one unbalanced triangles. The possible triangles are shown in Figure 2.1.

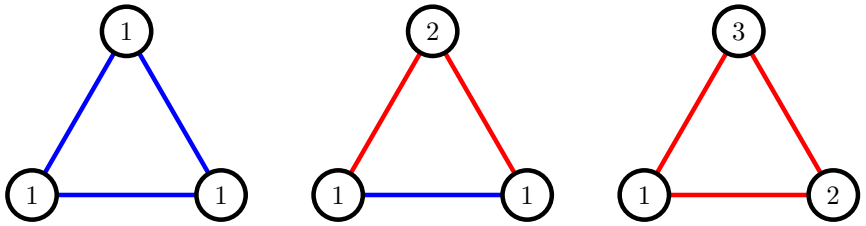

(a) $[+++]$ (b) $[--+]$ (c) $[---]$

Figure 2.1: Three possible triangles. Nodes (legislators) are represented as circles, and the number inside each of them correspond to the chosen vote option. Blue lines are positive links, and occur when two MP's voted the same. Red lines are the negative ones, which are present between nodes with different votes.

2.3 Counting links and triangles

As we said in the previous section, links and triangles are considered as spins or spin-like quantities in our proposed model. A central part of it consist on counting these amounts. At first, knowing them can allow us to measure the probability of choosing

a negative sign link or a balanced triangle randomly in a given network. But also, as we are going to show in following sections, it will let us construct physical quantities.

Since the network in model is fully connected, is easy to see it will have

$$L = \binom{N}{2} = \frac{N(N-1)}{2} \tag{2.2}$$

links and

$$C = \binom{N}{3} = \frac{N(N-1)(N-2)}{6} \tag{2.3}$$

triangles. Now, we also want to count the number of positive and negative links, and the amount of each type of triangle ($[+++]$, $[+--]$, and $[---]$).

Although we could have expressed these for the specific case of $k = 3$, as we mentioned above, we wanted to express these quantities in a generalized enough form not to rely on a particular number of options. For now on, we are going to refer to the vote options as partitions (or groups) because legislators can be said to to be gathered on groups according to what they voted.

In a similar way as for L and C, we are going to use combinatorics for counting the number of edges of different signs and triangles of different balance (and type). For each of the following quantities, we are going to show first a conceptualization of how we can count them. As we will see, the these raw counts will involve summations across independent and non overlapping indexes, which would translate on `for` loops when it came to count these amounts on a computer. This has the problem of being bad when scaling, meaning for high values of k the algorithms would perform inefficiently. To address this, we will work on the resulting expressions to get equivalent but cleaner forms, avoiding summations if possible.

Links

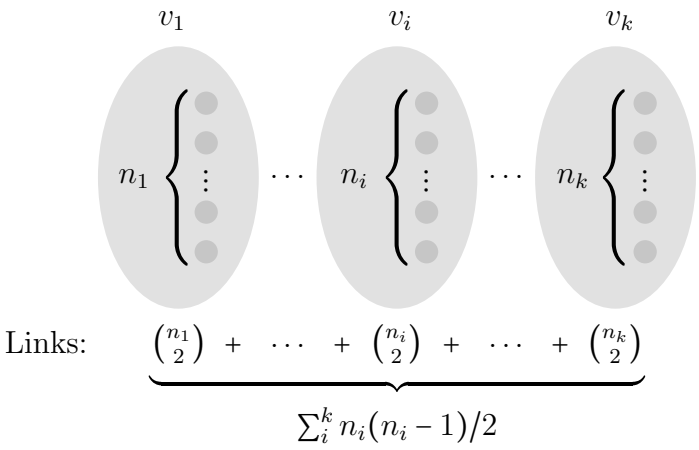

Figure 2.2: Counting links within each partition.

It is easy to see that the number of unsigned links is going to be the sum of the number of links within every partition. It can be denoted as $\sum_i^k n_i(n_i-1)/2$, whose numerator can be expanded and their sum split to get $\sum_i^k n_i^2/2 - \sum_i^k n_i/2$. From equation (2.1) and noting $\sum_i^k n_i^2$ is the euclidean norm of $\vec{n}$, squared, we get the amount of positive links is

$$\begin{aligned} L^+ &= \frac{1}{2}\sum_i^k n_i^2 - \frac{1}{2}\sum_i^k n_i \\ &= \frac{1}{2}\|\vec{n}\|^2 - \frac{N}{2}. \end{aligned} \tag{2.4}$$

Signed links, on the other hand, are going to be the result of taking each pair of groups, multiply the number of nodes inside each of them, and finally adding all those products. As is shown on Figure 2.3, L^- results in $\sum_{i<j}^k n_i n_j$. Notice this sum is equivalent to sum all the entries of the matrix $\vec{n} \otimes \vec{n}$ above its diagonal, which can also be expressed as the sum of all of the entries of that matrix minus the diagonal elements, divided by 2, since it is symmetric. All this can be pictured in Figure 2.4.

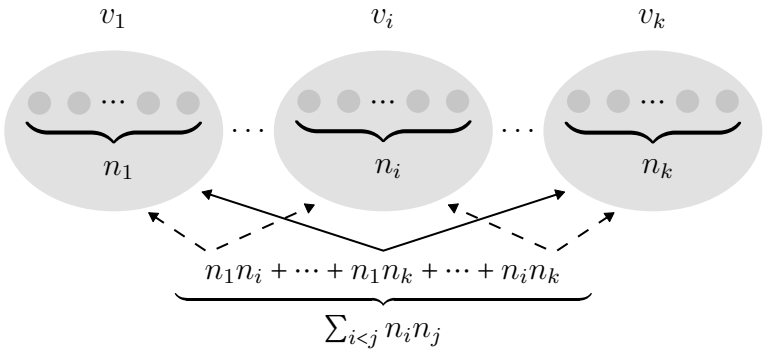

Figure 2.3: Counting links between different groups. Here v's are vote options.

The advantage of summing all the entries of such matrix is that we can write that as $\sum_i^k \sum_j^k n_i n_j = \sum_i^k n_i \sum_j^k n_j$, what then, from equation (2.1), results on N^2. Finally, the number of negative links will be

$$L^- = \frac{N^2}{2} - \frac{1}{2}\|\vec{n}\|^2 \tag{2.5}$$

Triangles

Counting the triangles takes a bit more work. Similar as for positive links, the number of triangles of type $[+++]$ is going to be equal to the sum of triangles inside each group, $\sum_a^k n_a(n_a-1)(n_a-2)/6$. If we expand and split the sum, there are going to arise terms with N and $\|\vec{n}\|^2$ again, but this time we are also going to have a new term with $\sum_a^k n_a^3$ on it. That part of such term will be noted as $\|\vec{n}\|_3^3$, since it is indeed the 3-norm of $\vec{n}$, cubed. Hence, the network will have

$$C_{+++} = \frac{1}{6}\left[\|\vec{n}\|_3^3 - 3\|\vec{n}\|^2 + 2N\right], \tag{2.6}$$

triangles of this type.

Now, for the $[---]$ triangles we have to consider that all the three nodes on each of these triangles must be on different groups. Then, there are going to be $\sum_{a<b<c}^k n_a n_b n_c$

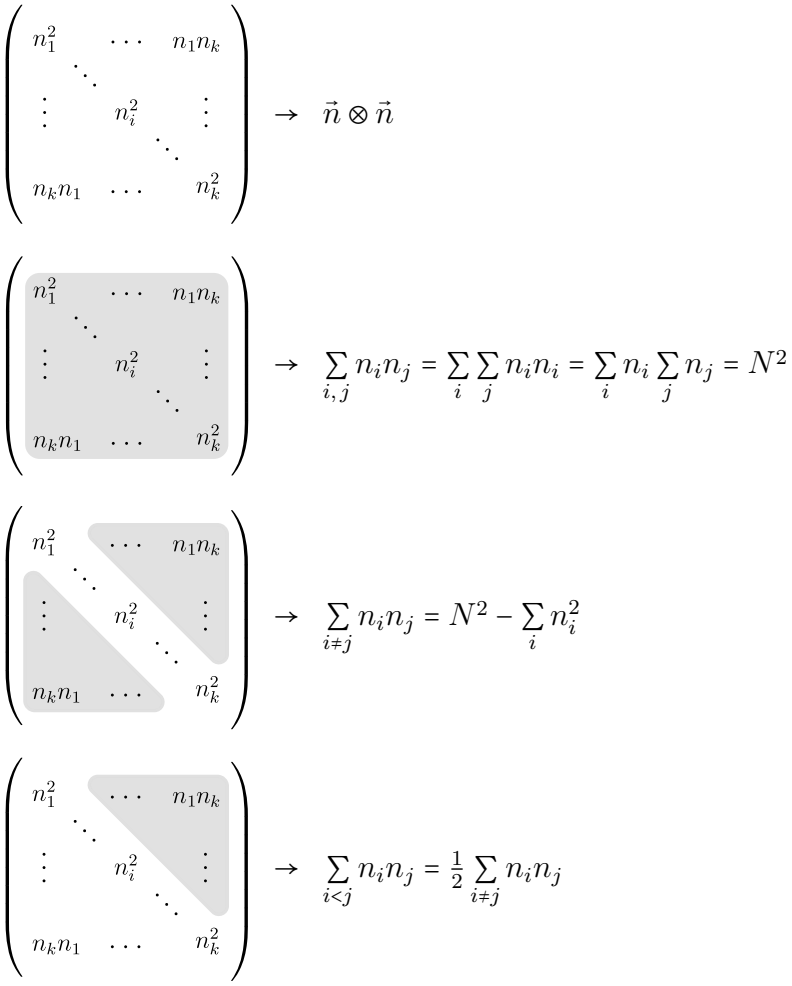

Figure 2.4: Summing entries of $\vec{n} \otimes \vec{n}$. Greyed out entries are taken into account for the sums.

of them, which can be simplified similarly as we did for $\sum_{i<j}^{k} n_i n_j$ above. In this case, instead of using the $\vec{n} \otimes \vec{n}$ matrix, we will use the $\vec{n} \otimes \vec{n} \otimes \vec{n}$ cube. A representation of it is shown on Figure 2.5.

Summing all this cube's entries can be represented as $\sum_{a,b,c}^{k} n_a n_b n_c$ and also is equal to N^3. Since we are looking for $\sum_{a<b<c}^{k} n_a n_b n_c$, we consider C_{---} as N^3 minus all the terms that are not the product of three different components of $\vec{n}$. But, by doing that we would be overcounting what we are looking for. As shown on Figure 2.6, each of these wanted terms appear six times, so, we have to divide the count by six to avoid this redundancy.

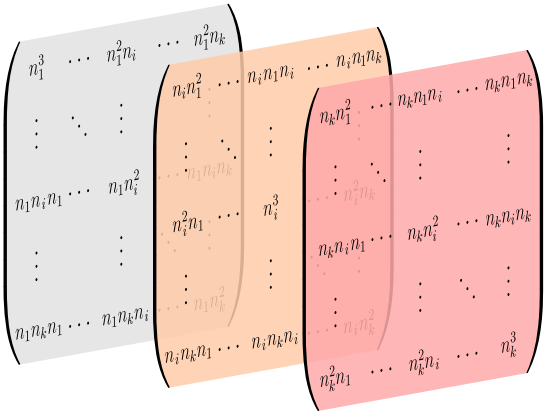

Figure 2.5: A representation of the $\vec{n}\otimes\vec{n}\otimes\vec{n}$ cube. Only three layers are drawn, but they represent a k amount of them.

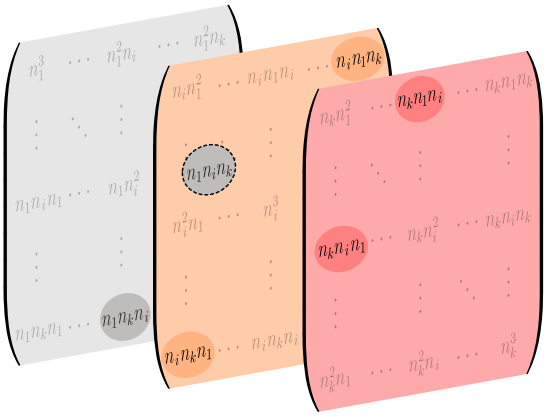

Figure 2.6: Products of three different components of $\vec{n}$ highlighted on the $\vec{n}\otimes\vec{n}\otimes\vec{n}$ cube.

Noting the sum of all these "not-wanted" terms we just said we have to subtract as NWT, we can summarize that —at this point— the amount of $[---]$ triangles is $\frac{1}{6}[N^3 - \text{NWT}]$.

Now, we will show that

$$\text{NWT} = \sum_a n_a^3 + 3\sum_{a\neq b} n_a^2 n_b. \tag{2.7}$$

Here, the first sum can be recognized as the diagonal of the cube (Figure 2.7), which for now on we will note as $\|\vec{n}\|_3^3$.

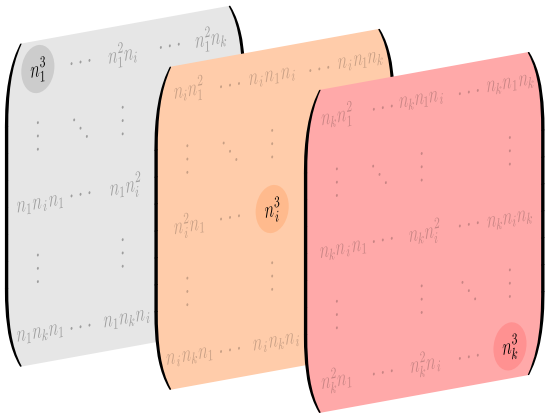

Figure 2.7: Diagonal of the cube $\vec{n} \otimes \vec{n} \otimes \vec{n}$.

About the second sum on equation (2.7), if we take a look on the terms where two indexes coincide we get that for distinct pairs a, b, each $n^2 n_b$ term appears three times, being this the reason for the factor before the summation. This is pictured on Figure 2.8, and can also be noted considering that a term $n_a^2 n_b$ could be the result of $n_a n_a n_b, n_a n_b n_a$, and $n_b n_a n_a$. Now, leaving the factor of 3 aside for a moment,

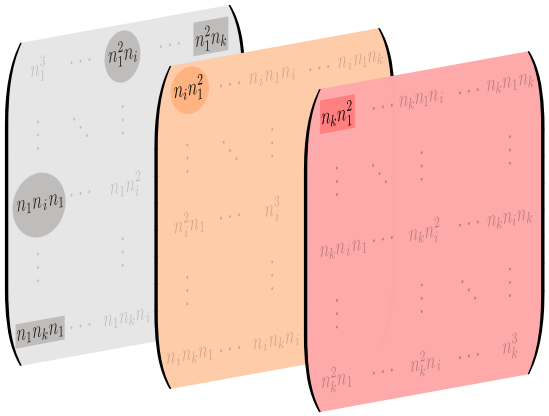

Figure 2.8: Terms with the form $n_a^2 n_b$, for $a = 1$ and $b \in \{1, \ldots, k\}$, highlighted in the $\vec{n} \otimes \vec{n} \otimes \vec{n}$ cube. Terms for $b = 1$ are highlighted in circles, while in rectangles for $b = k$. It can be seen that each of them appear three times.

from what is shown next to the third matrix on Figure 2.4, we can realize that $\sum_{i \neq j}^{k} \bigcirc_{ij} = \sum_{i}^{k} \sum_{j}^{k} \bigcirc_{ij} - \sum_{i}^{k} \bigcirc_{ii}$. Applying this to $\sum_{a \neq b} n_a^2 n_b$ would yield us this sum is equal to $\sum_{a}^{k} \sum_{b}^{k} n_a^2 n_b - \sum_{a}^{k} n_a^3 = N \|\vec{n}\|^2 - \|\vec{n}\|_3^3$.

Considering all this, we have that

$$\begin{aligned} C_{---} &= \sum_{a<b<c}^{k} n_a n_b n_c \\ &= N^3 - \|\vec{n}\|_3^3 - 3\left(N\|\vec{n}\|^2 - \|\vec{n}\|_3^3\right), \end{aligned}$$

which results on

$$C_{---} = \frac{1}{6}\left[N^3 + 2\|\vec{n}\|_3^3 - 3N\|\vec{n}\|^2\right]. \tag{2.8}$$

Finally, for the $[+--]$ type triangles, we compute the amount of possible combinations of three nodes with two of them being in the same group while the third belongs to another.

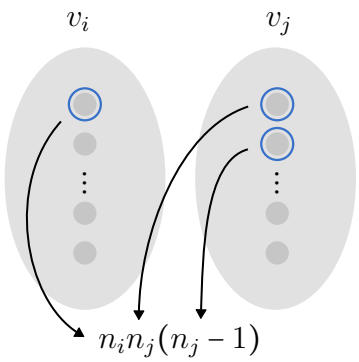

Figure 2.9: Counting triangles with two nodes being in the same group while the third belongs to another.

As can be seen on Figure 2.9, it gives us $n_i n_j (n_j - 1)$, but we also have to consider the other way around, where the two nodes are in the i-labeled group and the remaining one is in the j-labeled group, which in this case is $n_j n_i (n_i - 1)$. We want to sum this over all distinct pair of vote options v_i and v_j, so the summation goes like $\sum_{i<j}^{k} n_i n_j (n_j - 1) + n_j n_i (n_1 - 1)$, but we also have to divide this by 2 for taking the permutations the two nodes that belong to the same group have into account. Note that, if we distribute the sum and interchange the index labels for the second

term, we get

$$\begin{aligned}\sum_{i<j}^{k}\frac{n_i n_j(n_j-1)+n_j n_i(n_1-1)}{2} &= \frac{1}{2}\left[\sum_{i<j}^{k} n_i n_j(n_j-1)+\sum_{j<i}^{k} n_i n_j(n_j-1)\right]\\ &= \frac{1}{2}\sum_{i\neq j}^{k} n_i n_j(n_j-1)\\ &= \frac{1}{2}\left[\sum_{i}^{k}\sum_{j}^{k} n_i n_j(n_j-1)-\sum_{i}^{k}(n_i^3-n_i^2)\right]\\ &= \frac{1}{2}\left[N(\|\vec{n}\|^2-N)-\|\vec{n}\|_3^3+\|\vec{n}\|^2\right].\end{aligned}$$

Here we have used the fact that a sum like $\sum_{i<j}\bigcirc_{ij}$ plus a sum $\sum_{j<i}\bigcirc_{ij}$ is equal to $\sum_{i\neq j}^{k}\bigcirc_{ij}$ or $\sum_{i}^{k}\sum_{j}^{k}\bigcirc_{ij}-\sum_{i}^{k}\bigcirc_{ii}$. This can also be observed in Figure 2.4. Then, we got

$$C_{+--}=\frac{1}{2}\left[(N+1)\|\vec{n}\|^2-\|\vec{n}\|_3^3-N^2\right] \tag{2.9}$$

is the amount of triangles of this type in the network.

It can be seen that the number of balanced triangles is going to be C_{+++} plus C_{+--}, so, hereafter, we are going to denote this as C^+, whose value is going to be

$$\begin{aligned}C^+ &= \frac{1}{6}\left[\|\vec{n}\|_3^3-3\|\vec{n}\|^2+2N\right]+\frac{1}{2}\left[(N+1)\|\vec{n}\|^2-\|\vec{n}\|_3^3-N^2\right]\\ &= \frac{1}{6}\left[\|\vec{n}\|_3^3-3\|\vec{n}\|^2+2N+3N\|\vec{n}\|^2+3\|\vec{n}\|^2-3\|\vec{n}\|_3^3-3N^2\right]\\ &= \frac{1}{6}\left[2(N-\|\vec{n}\|_3^3)+3N(\|\vec{n}\|^2-N)\right]=\frac{1}{6}\left[N(2+3(\|\vec{n}\|^2-N))-2\|\vec{n}\|_3^3\right]\end{aligned} \tag{2.10}$$

Also, we will refer as C^- to the amount of $[---]$ triangles (C_{---}) as well, since those are the only triangles that are unbalanced.

2.4 Magnetizations and energy

In this section we are going to define what we are going to consider as magnetizations. First of all, we are going to define two of them. One for the links (M_ℓ) and another for the triangles (M_t). Both will have similar definitions, varying almost only on their dependence on the amount of (un)signed links or (un)balanced triangles, accordingly.

Finally, an energy function or Hamiltonian will be proposed, while assuring its minimization makes sense for our system, in the context of social fragmentation or polarization.

Magnetization

Magnetizations are going to be treated similar to average magnetization in the Ising model. They will be the number of positive sign spins minus the number of negative sign spins, over the total number of spins. We are going to note them with lowercase "m". But, for the sake of a good and clear presentation of these, let us define first the un-normalized magnetizations as follows. These last will be noted with upper M.

For links we have that

$$M_\ell = L^+ - L^-, \tag{2.11}$$

and for triangles that

$$M_t = C^+ - C^-. \tag{2.12}$$

Given we already have expressions for L^+, L^-, C^+, and C^- from equations (2.4), (2.5), (2.8) and (2.10), we evaluate them on equations (2.11) and (2.12). Then, the first

results on

$$\begin{aligned} M_\ell &= \left(\frac{1}{2}\|\vec{n}\|^2 - \frac{N}{2}\right) - \left(\frac{N^2}{2} - \frac{1}{2}\|\vec{n}\|^2\right) \\ &= \|\vec{n}\|^2 - \frac{N(N+1)}{2}, \end{aligned} \tag{2.13}$$

while the latter on

$$\begin{aligned} M_t &= C^+ - C^- \\ &= \frac{1}{6}\left[2(N - \|\vec{n}\|_3^3) + 3N(\|\vec{n}\|^2 - N)\right] - \frac{1}{6}\left[N^3 + 2\|\vec{n}\|_3^3 - 3N\|\vec{n}\|^2\right] \\ &= \frac{1}{6}\left[2N - 4\|\vec{n}\|_3^3 + 6N\|\vec{n}\|^2 - 3N^2 - N^3\right]. \end{aligned} \tag{2.14}$$

Finally, their average magnetizations (or magnetizations per spins) are going to be $m_\ell = M_\ell/L$ and $m_t = M_t/C$.

Both quantities expressed on equations (2.13) and (2.14) would communicate (indirectly) how much are legislators agreeing with each other. The closer the average magnetizations (m_ℓ and m_t) get to 0, the more disagreement or frustration will be on the system. If they lean toward 1 it would mean there are more positive links or balanced triangles than their oposite counterparts. Naturally, if the average tend to -1 it would be the oposite.

Hamiltonian

Putting the magnetizations aside, now we are going to define our energy function. We want this to be an extensive quantity, meaning the global energy of the system should be equal to the sum of the system elements energies. Ideally, the energy of elements of different type should differ. Finally, as we mentioned earlier, we want

the minimization of this to mean something appropriate.

Specifically, we want the energy of the system be minimum when everyone agrees with each other i.e. what it is called *utopia* by Heider [61]. In other terms, in this scenario the network would have all its links with +1 on their values, thus, all its triangles will be balanced. Also, the average link and triangle magnetizations m_ℓ and m_t will be 1.

For this, for a single triangle t we have defined the energy function h as

$$h(t) = -\sum_{\text{sides of } t} \text{sign of the side} \tag{2.15}$$

which is the negative sum of their sides. This would lead us to

$$h(+++) = -3, \qquad h(+--) = -1, \qquad h(---) = 3, \tag{2.16}$$

for each triangle type.

Then, the energy function for the whole system, or Hamiltonian, would be

$$\begin{aligned} H &= \sum_{t \in \text{triangles}} h(t) \\ &= -\sum_{\substack{t \\ \text{triangles}}} \sum_{\substack{s \\ \text{sides of } t}} \text{sign of } s. \end{aligned} \tag{2.17}$$

It is clear that with equation (2.16) we achieve that each triangle type have its own "energy", allowing us to distinguish them. Also, in equation (2.17) our energy minimization goal is fulfilled. When all the triangles are balanced H is on its minimum value.

Alternative form for the energy

Now we are going to show that the Hamiltonian we just presented can also be expressed in a different but equivalent way.

Since the outer sum on equation (2.17) is along all triangles, the whole expression its equivalent to count the number of triangles of each type and pondered them by their respective energy. All this times -1.

$$H = -\Big[h(+++)C_{+++} + h(+--)C_{+--} + h(---)C_{---}\Big] \tag{2.18}$$

Hereunder we are going to develop equation (2.18) using the amount of each triangle type and their associated energies, from equations (2.6), (2.8), (2.9) and (2.16).

$$\begin{aligned} H = -\Bigg[& (3)\,\frac{1}{6}\Big[\|\vec{n}\|_3^3 - 3\|\vec{n}\|^2 + 2N\Big] \\ & +(-1)\,\frac{1}{2}\Big[(N+1)\|\vec{n}\|^2 - \|\vec{n}\|_3^3 - N^2\Big] \\ & +(-3)\,\frac{1}{6}\Big[N^3 + 2\|\vec{n}\|_3^3 - 3N\|\vec{n}\|^2\Big] \Bigg], \end{aligned}$$

is what we got. Note the $\|\vec{n}\|_3^3$ terms (in red) cancel out. Then, we get

$$\begin{aligned} H = -\Bigg[& (3)\,\frac{1}{6}\Big[-3\|\vec{n}\|^2 + 2N\Big] \\ & +(-1)\,\frac{1}{2}\Big[(N+1)\|\vec{n}\|^2 - N^2\Big] \\ & +(-3)\,\frac{1}{6}\Big[N^3 - 3N\|\vec{n}\|^2\Big] \Bigg] \end{aligned}$$

where we can factorize the $\|\vec{n}\|^2$ terms (in blue) and rearange as follows:

$$\begin{aligned} H &= -\left[\|\vec{n}\|^2\left(-\frac{3}{2}-\frac{1}{2}(N+1)-\frac{3}{2}N\right)+N+\frac{N^2}{2}-\frac{N^3}{2}\right], \\ &= -\left[\|\vec{n}\|^2\frac{1}{2}\big(N-2\big)-\frac{N}{2}\Big(N^2-N-2\Big)\right], \\ &= -\left[\|\vec{n}\|^2\frac{1}{2}\big(N-2\big)-\frac{N}{2}\Big(N-2\Big)\Big(N+1\Big)\right]. \end{aligned}$$

Finally, we get

$$H = -(N-2)\frac{1}{2}\left[2\|\vec{n}\|^2 - N(N+1)\right]. \tag{2.19}$$

Note that, from equations (2.4), (2.5) and (2.11), in equation (2.19), every factor but $-(N-2)$ is equal to M_ℓ. So, the whole expression results

$$H = -(N-2)M_\ell. \tag{2.20}$$

Another way to obtain this expression is noting that in equation (2.17), apart from multiplying everything by -1, we are summing each link value $N-2$ times, since that is the amount of triangles each link is in —in our fully-connected network. Considering this, we could write the Hamiltonian as

$$H = -(N-2)\sum_{\substack{\ell \\ \cap \\ \text{links}}} \ell, \tag{2.21}$$

and since links values are just 1 or -1, that sum is equivalent to count the difference between the (1)-valued and (-1)-valued links i.e. the magnetization M_ℓ. Doing this, as expected, we recover equation (2.20).

2.5 Entropies

In this section we present two entropies. One for links and one for triangles. Both are defined almost identically, with minor difference on their dependence of the amount of each type of links or triangle, accordingly. Following, we are going to derived the expressions in two different ways, starting with Boltzmann and Shannon definitions of entropy, which also are going to hint us different interpretations these entropies can have.

Using Boltzmann entropy

Lets recall we are proposing a framework using the microcanonical ensamble, so, for a fixed network configuration $\vec{n}$, all microstates must have the same probability. Here, the microstates are going to be possible internal configurations the network could be in order to have k groups with their size described by $\vec{n}$.

If the number of microstates is $\Omega_{\vec{n}}$ for a specific configuration $\vec{n}$, then the probability of occurrence for each one is $1/\Omega_{\vec{n}}$. But, it is important to note that the amount of microstates is going to be different whether we take links or triangles as spins. To distinguish these quantities we are going to note with ℓ or t as super-index, when regarding to links or triangles, respectively.

While treating links as spins, this amount will be

$$\Omega^{\ell}_{\vec{n}} = \frac{L!}{L^{+}!L^{-}!}, \tag{2.22}$$

where only L^{+} and L^{-} depend on $\vec{n}$. Now we evaluate the Boltzmann entropy

$$S = k_B \ln(\Omega) \tag{2.23}$$

with $\Omega = \Omega^{\ell}_{\vec{n}}$. This results on

$$S_\ell = -k_B \ln\left(\frac{L^+!\, L^-!}{L!}\right),$$

where we use the Stirling approximation for the logarithm of factorials. Then, it leads us to

$$\begin{aligned} S_\ell &= -k_B \left[L^+ \ln(L^+) + L^- \ln(L^-) - L\ln(L) - L^+ - L^+ + L\right] \\ &= -k_B \left[p^+_\ell L \ln(p^+_\ell L) + p^-_\ell L \ln(p^-_\ell L) - L\ln(L)\right], \end{aligned}$$

where the terms in red cancel out, yielding us

$$S_\ell = -k_B L\Big[p^+_\ell \ln(p^+_\ell) + p^-_\ell \ln(p^-_\ell)\Big], \tag{2.24}$$

with $p^+_\ell = L^+/L$ and $p^-_\ell = L^-/L$ the probabilities of a link of being unsigned or signed, respectively. Following the same line of thought, for triangles we would have

$$S_t = -k_B C \left[p^+_t \ln(p^+_t) + p^-_t \ln(p^-_t)\right], \tag{2.25}$$

now, with $p^+_t = C^+/C$ and $p^-_t = C^-/C$ the probabilities of a triangle of being balanced or not.

Please note that, in equations (2.24) and (2.25), the probabilities $p^+_\ell, p^-_\ell, p^+_t$, and p^-_t will have different values for different vote scenarios/network configurations ($\vec{n}$). In other words, these are not constant across the configuration space.

Using Shannon entropy

Employing Shannon's definition of entropy it is more direct in this case. First, we recall that the definition is

$$S = -k_B D \sum_{s\,\in\,\text{states}} p^s \ln p^s, \tag{2.26}$$

where D is the total number of spins and p^s are the probabilities of finding a spin on a state s.

So, if we take the case of links, they have only two possible states. Unsigned and signed, which correspond to values 1 or -1. Then, we are only going to have the probabilities p_ℓ^+ and p_ℓ^-. Consequently, if we take this, and also replace D with L, into equation (2.26), we would get that the link entropy will be equal to S_ℓ in equation (2.24) as well.

In the case of triangles, if we consider as the states as being balanced or unbalanced, the mathematical development is going to be the same as for links (but with p_t instead of p_ℓ, and C instead L), obtaining also S_t as in equation (2.25).

However, for triangles there is another entropy we could build from this definition of entropy. If we take the triangle types for states rather than the balancedness, then triangles would have three states rather than just two. The resulting entropy is going to be

$$\tilde{S}_t = -k_B C\Big[p_t^{+++}\ln(p_t^{+++}) + p_t^{+--}\ln(p_t^{+--}) + p_t^{---}\ln(p_t^{---})\Big], \tag{2.27}$$

where p_t^{+++}, p_t^{+--} and p_t^{---} are going to be the probabilities of finding a triangle of each type in a given network. As it was expressed on equation (2.27), we are going to refer to this variant entropy for triangles as $\tilde{S}_t$, to distinguish it from the already-mentioned entropy S_t.

Entropy in terms of magnetization

In this section we show that it is possible to write the entropies S_ℓ and S_t in terms of the magnetizations. For this, we just need to express the probabilities $p_\ell^+, p_\ell^-, p_t^+$, and p_t^- in term of their respective magnetizations m_ℓ and m_t, and put them on equations (2.24) and (2.25).

Let's start with the fact that the normalized link magnetization is

$$m_\ell = \frac{L^+ - L^-}{L} = \frac{L^+}{L} - \frac{L^-}{L} = p_\ell^+ - p_\ell^-.$$

Now, if we also take that $p_\ell^+ + p_\ell^- = 1$, we can add or subtract this 1 to m_ℓ, to isolate p_ℓ^+ or p_ℓ^-. That way, it yield us that the links probabilities are

$$p_\ell^+ = \frac{1}{2}(1 + m_\ell), \tag{2.28}$$

and

$$p_\ell^- = \frac{1}{2}(1 - m_\ell). \tag{2.29}$$

For the triangle probabilities is going to be analogous:

$$p_t^+ = \frac{1}{2}(1 + m_t), \tag{2.30}$$

$$p_t^- = \frac{1}{2}(1 - m_t). \tag{2.31}$$

Thus, replacing equations (2.28) and (2.29) on equation (2.24), and equations (2.30) and (2.31) on equation (2.25), the entropies result

$$S_\ell = -L\,k_B\left[\left(\frac{1+m_\ell}{2}\right)\ln\left(\frac{1+m_\ell}{2}\right) + \left(\frac{1-m_\ell}{2}\right)\ln\left(\frac{1-m_\ell}{2}\right)\right] \tag{2.32}$$

and

$$S_t = -C\,k_B\left[\left(\frac{1+m_t}{2}\right)\ln\left(\frac{1+m_t}{2}\right) + \left(\frac{1-m_t}{2}\right)\ln\left(\frac{1-m_t}{2}\right)\right], \tag{2.33}$$

for links and triangles, respectively.

Hereinafter, we are going to refer as entropies as the normalized entropies or average entropy per amount of spins, and we are going to note them with lowercase

"s". These will be

$$s_\ell = \frac{S_\ell}{L}, \qquad s_t = \frac{S_t}{C}, \qquad \tilde{s}_t = \frac{\tilde{S}_t}{C}. \tag{2.34}$$

2.6 Temperature

In this section we define a temperature for the system, whose interpretation is going to be rooted on the thermodynamic definition of temperature

$$\frac{1}{T} = \left(\frac{\partial S}{\partial U}\right)_N \tag{2.35}$$

where T is the temperature, S the entropy, N the number of particles, and U the internal energy. In this definition we have omitted the constrain of fixed volume because as we deal with a spins system, it does not apply.

Note we already have and expression for S_ℓ in terms of m_ℓ on equation (2.32). In addition, from equation (2.20), we can write m_ℓ in terms of H, as $m_\ell = \frac{-H}{L(N-2)}$. So, we can say equation (2.35), for the entropy S_ℓ, follows as

$$\frac{1}{T} = \frac{\partial S_\ell}{\partial m_\ell}\frac{\partial m_\ell}{\partial H}, \tag{2.36}$$

where we have considered the internal energy U as H. Then, evaluating the partial derivative $\frac{\partial m_\ell}{\partial H}$, it goes as

$$\frac{1}{T} = \frac{-1}{L(N-2)}\frac{\partial S_\ell}{\partial m_\ell}. \tag{2.37}$$

Meanwhile, to compute the remaining partial derivate we differentiate equation (2.32) with respect to m_ℓ. This results on

$$\frac{\partial S_\ell}{\partial m_\ell} = -\frac{1}{2}\ln\left(\frac{1+m_\ell}{1-m_\ell}\right) L\, k_B. \tag{2.38}$$

Finally, using this on equation (2.37) yields

$$\frac{\partial H}{\partial S_\ell} = (N-2)L\left[\frac{1}{2}\ln\left(\frac{1+m_\ell}{1-m_\ell}\right)L\,k_B\right]^{-1},$$

where the L factors (in red) simplify, thus, the temperature results in

$$T = (N-2)\frac{2}{k_B}\left[\ln\left(\frac{1+m_\ell}{1-m_\ell}\right)\right]^{-1}. \tag{2.39}$$

Additional relations with temperature

With the expression for T itself we can start expressing other quantities in terms of T. Specifically, we want to write the magnetization and the Hamiltonian in terms of it for a later analysis on these relations.

To get m_ℓ on terms of T we need to isolate it from equation (2.39). On that expression, accommodating T and the logarithm, we get that

$$\ln\left(\frac{1+m_\ell}{1-m_\ell}\right) = (N-2)\frac{2}{Tk_B}.$$

Now we apply the exponential function on each side and rearrange the terms and factors as follows.

$$\begin{aligned}
\frac{1+m_\ell}{1-m_\ell} &= e^{\frac{2(N-2)}{Tk_B}},\\
1+m_\ell &= (1-m_\ell)e^{\frac{2(N-2)}{Tk_B}},\\
m_\ell\left(1+e^{\frac{2(N-2)}{Tk_B}}\right) &= e^{\frac{2(N-2)}{Tk_B}}-1,\\
m_\ell &= \frac{1-\left(e^{-\frac{1}{T}}\right)^{\frac{2(N-2)}{k_B}}}{\left(e^{-\frac{1}{T}}\right)^{\frac{2(N-2)}{k_B}}+1}.
\end{aligned}$$

If we look carefully we can note this have the form of an hyperbolic tangent of $\frac{1}{T}$.

Concretely, this equals

$$m_\ell = \tanh\left(\frac{N-2}{k_B T}\right). \tag{2.40}$$

Finally, recalling that $M_\ell = L\, m_\ell$ and using equation (2.40) on equation (2.20), the Hamiltoninan yield us

$$H = -(N-2)L \tanh\left(\frac{N-2}{k_B T}\right). \tag{2.41}$$

With this we end the presentation of the model. Summarizing, we have successfully derived a microcanonical formalism for a signed agreement network of legislators. Our network is fully-connected and each link value takes relation with whether both parliamentarians voted the same or not. We based on balanced theory for focusing on triangle balance and taking them as spins, while at the same time we also did that for the links signs.

Four major physical magnitudes have been derived for this system. We started with magnetizations for links and triangles, which were followed by entropies for those spin types as well. For this, we counted the amount of links and triangles of each kind, exactly, taking advantage of the network being completely connected while deriving mathematical expressions for these cardinalities.

We also introduced a Hamiltonian looking its minimization would mean the complete agreement between the politicians, deriving two different approaches to obtain our final expression for it. Later, having this magnitud gave us rise to derive an expression for the temperature of the system, hanging on its thermodynamical definition, which relate the change on energy with the change on entropy. Finally, we also were able to express the Hamiltonian in terms of the temperature.

In the next chapter we are going to analyze the expressions we have derived on

this chapter, and will see how they behave analytically and when they are computed for a specific value of k and N.

Chapter 3

Model analysis

We have successfully derived a microcanonical formalism for the system at stake. Now, we are going to take a dive into the behaviour of the mathematical expressions presented in the previous chapter. For simplicity, on most of the following analysis we are going to assume $k = 3$, that is to say, we are going to consider that each vote only have three options: *for*, *against*, and *abstain*. We are also going to assume $N = 155$, in order to ease the later evaluation of the model with data that will be done in Chapter 4.

3.1 Configuration space for $k = 3$ and $N = 155$

In this case, the equation that fully describe this system is

$$n_1 + n_2 + n_3 = 155, \tag{3.1}$$

which actually is the equation (2.1) but with $k = 3$ and $N = 155$. This is plotted Figure 3.1 to take a picture of the phase space. Please note that, despite it looks like there is a continuous triangle, there is no such thing. If the reader look carefully

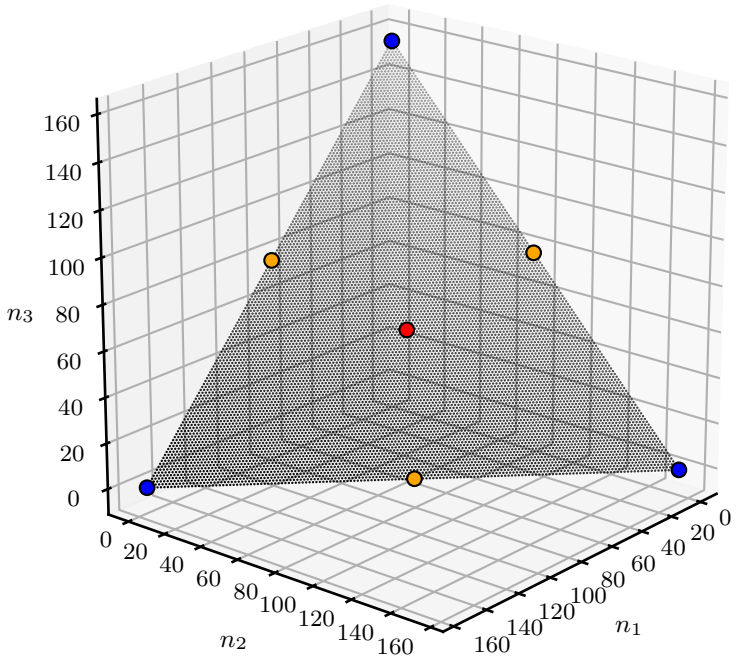

Figure 3.1: 3D representation of the phase space. Each black dot on this plane represent a possible vote scenario. Also, some specific vote scenarios are highlighted with bigger and coloured points.

the figure will see that the "triangle" is actually formed by tiny black dots, which are apart from each other i.e. we have plotted all solutions for for discrete values of n_1, n_2 and n_3, in the range $[0, 155]$.

3.2 Magnetizations and entropies

The next thing we are going to show is that we can plot most of the physical magnitudes from the previous section in on top of the configuration space. We can color the dots of Figure 3.1 according the values of theses quantities. For instance, on Figures 3.2 to 3.5 we have plotted the magnetizations and entropies, respectively.

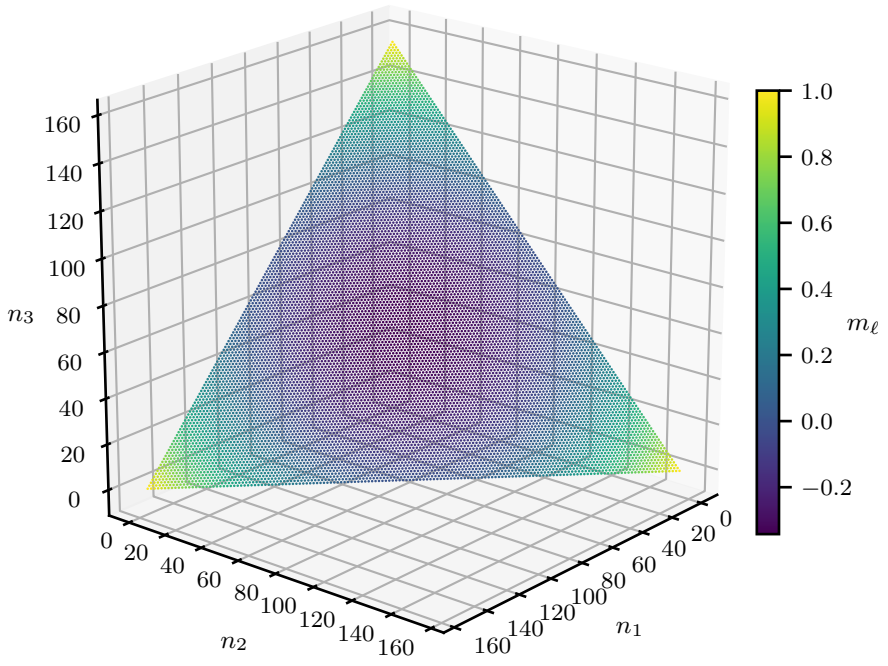

Figure 3.2: Link magnetization across different configurations on the configuration space.

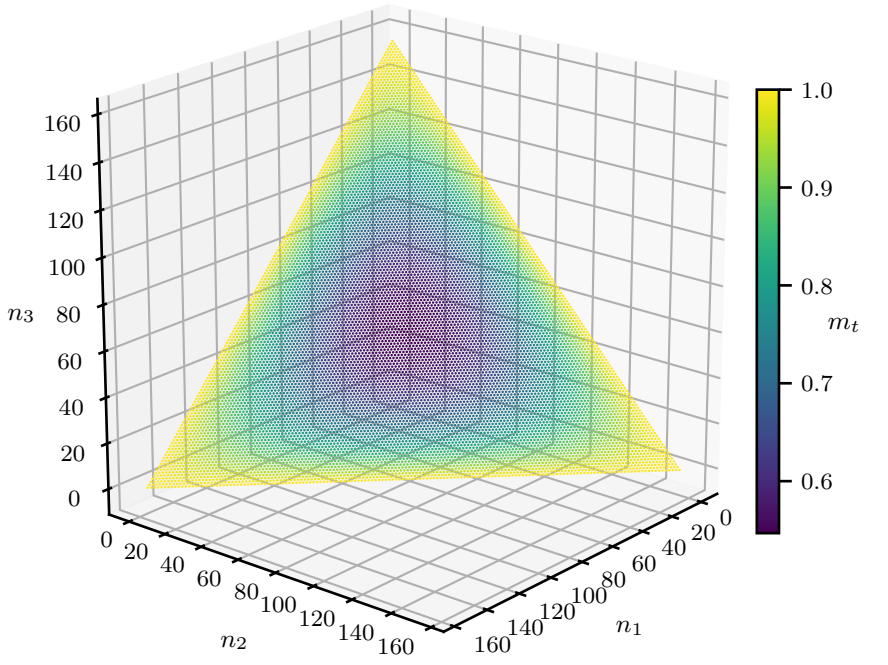

Figure 3.3: Triangle magnetization across different configurations on the configuration space.

At first glance, we can see that link magnetization leans higher values to (more) unanimous votes, towards the corners of the configuration space triangle. The triangle counterpart seems to not being able to distinguish between an unanimous agreement and votes mainly divided between two options —both cases where this has its maximum value $m_t = 1$.

On the other side, entropies seem the oposite of magnetizations. For example, maximums of Figure 3.3 correspond to minimums on Figure 3.5, and viceversa.

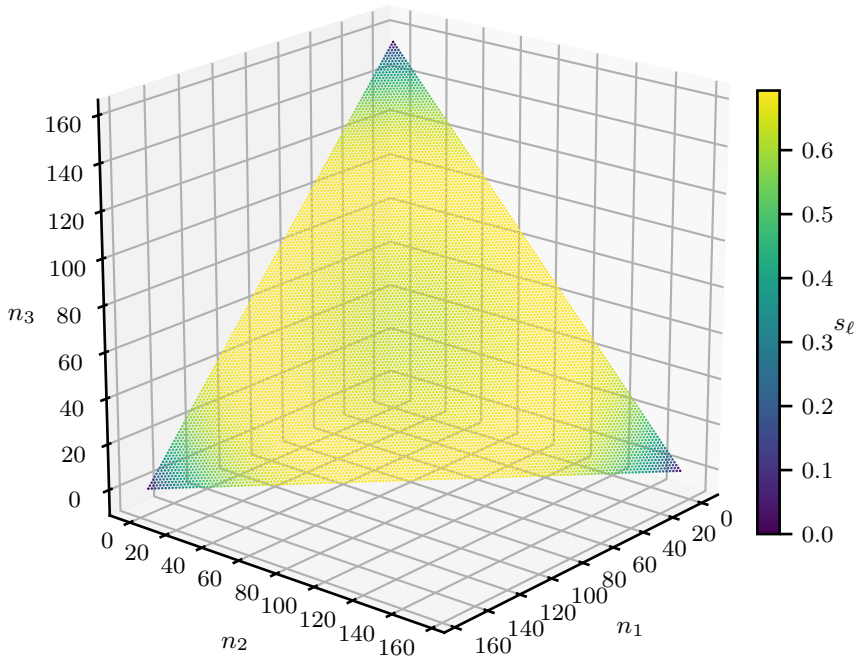

Figure 3.4: Link entropy across different configurations on the configuration space.

Nevertheless, while the minimum of the link magnetization (on Figure 3.2) is on the center of the configuration space, the maximum link entropy is not there. A more detained look up will show us that the center (of the configuration space) actually is a local minimum, and therefore it is surrounded by a neighbourhood of maximum entropy configurations. This can be better seen in Figure 3.6, where s_ℓ has been plotted on the vertical axis.

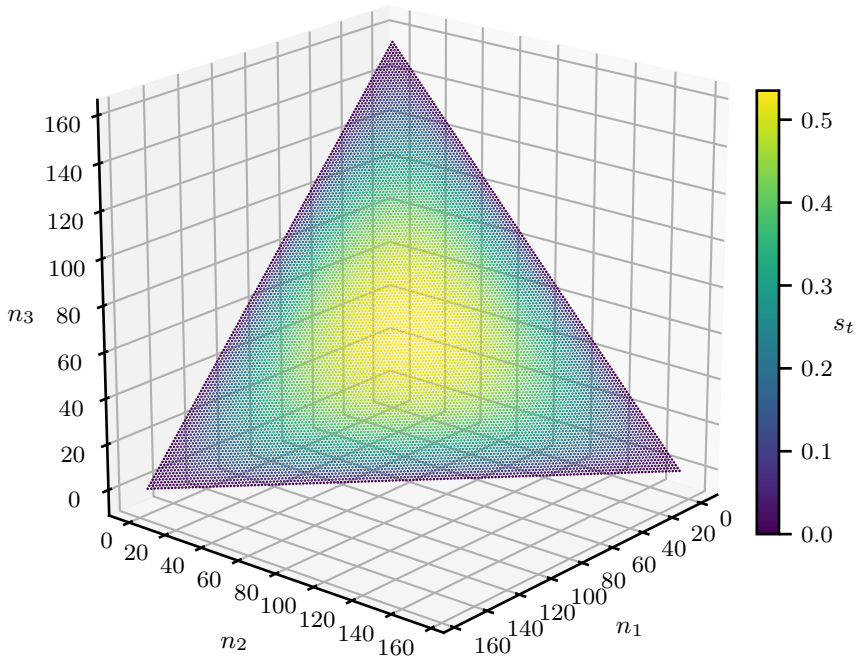

Figure 3.5: Triangle entropy across different configurations on the configuration space.

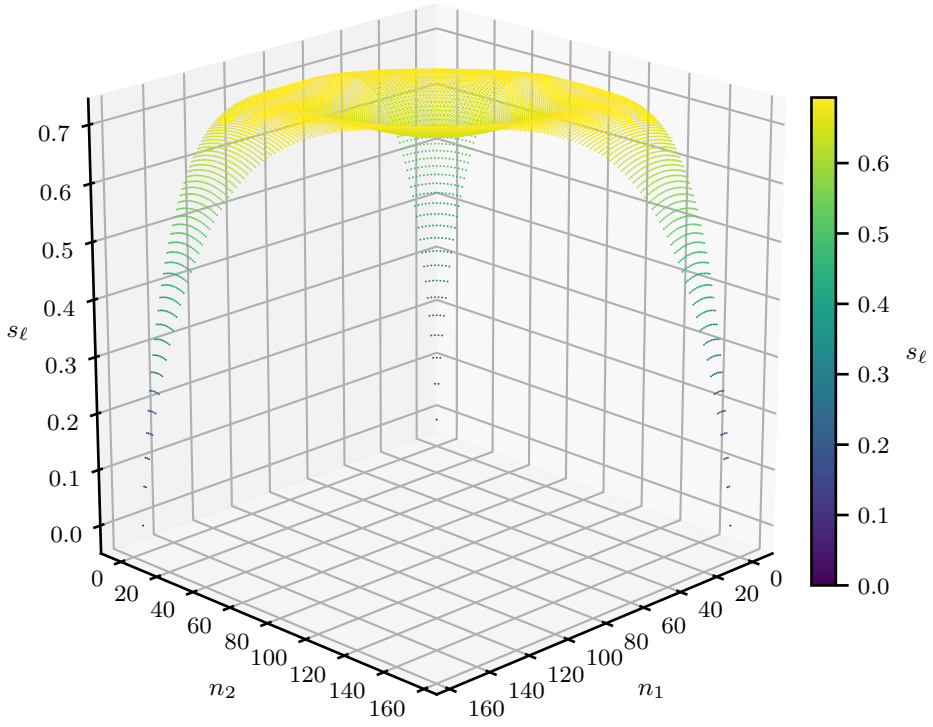

Figure 3.6: Link entropy plotted against how many legislator have chosen each of two vote options. The third options is derived from equation (2.1).

On Figure 3.7 we also plot the alternative triangle entropy $\tilde{S}_t$ presented on equation (2.34), which, as it can be seen, present three areas of high entropy where there is a maximum.

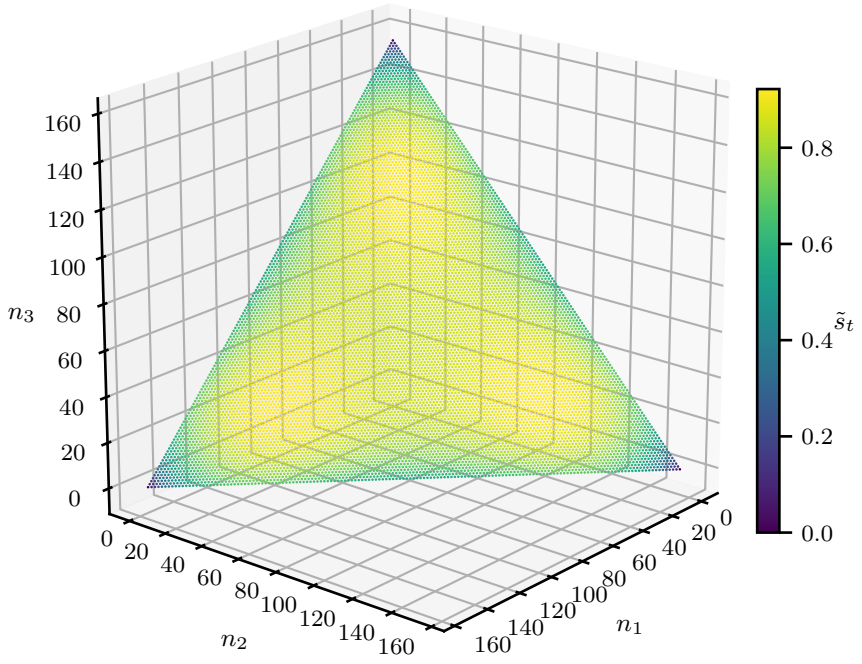

Figure 3.7: Alternative triangle entropy where the triangles types are the states rather than balancedness.

Minimum of m_ℓ and maximum of s_ℓ

Now we will solve analytically where are the minimum of m_ℓ and maximum of s_ℓ, for k amount of vote options, hoping to get expressions compatible with what we have just seen on Figures 3.2, 3.4 and 3.6.

We are going to start proving m_ℓ has its minimum of the center of the configuration space differentiating M_ℓ with respect to our generalized variables and stating that derivative is equal to zero. We use the value for M_ℓ we got from equation (2.13) and differentiate it with respect to each n_i, with $i \in \{1, \ldots, k\}$. While doing that, since $M_\ell = \frac{1}{2}\Big[2\|\vec{n}\|^2 - N(N-1)\Big]$, it can bee seen that $-N(N-1)$ remains constant,

so, our derivative will end up being just $\frac{\partial M_\ell}{\partial n_i} = \frac{\partial \|\vec{n}\|^2}{\partial n_i}$, leaving us with

$$\frac{\partial}{\partial n_i}\|\vec{n}\|^2 = 0 \tag{3.2}$$

at the end. Here we have written a derivative of $\|\vec{n}\|^2$ with respect to the number of any general vote option i, but it is important to remember that in order to identify a minimum taking the partial derivate with respect to all vote options —and equal them to zero— is needed. So, really, we will have to solve a system of equations. Also, it is important to consider equation (2.1) before differentiating because we only have $k-1$ independent variables. In other words, any of them can be expressed in terms of the others.

For the purpose of this computation, we are going to say the last dimension i.e. n_k is going to be $N - \sum_{i=1}^{k-1} n_i$. Putting this into equation (3.2) gives us

$$0 = \frac{\partial}{\partial n_i}\left[\left(\sum_{j=1}^{k-1} n_j^2\right) + \left(N - \sum_{j=1}^{k-1} n_j\right)^2\right].$$

Now, for the sake of order, in the following steps we are going to rewrite this expression with Einstein notation. We will drop each sum symbol and take each pair of repeated indexes as an implicit sum along them, from 1 to $k-1$. In order to accomplish this, the sum $\sum_{j=1}^{k-1} n_j$ will be noted as $n_j\sigma_j$, with σ_j being the j-th component of the vector $\mathbf{1} = \{1, 1, \ldots, 1\}$ of dimension $k-1$. Then, the expression from above turns

$$\begin{aligned} 0 &= \frac{\partial}{\partial n_i}\left[n_j n_j + \left(N - n_j\sigma_j\right)^2\right] \\ &= \frac{\partial}{\partial n_i}\left[n_j n_j + N^2 - 2N n_j\sigma_j + \left(n_j\sigma_j\right)^2\right]. \end{aligned} \tag{3.3}$$

Differentiating this, it yields

$$\begin{aligned} 0 &= 2\delta_{ij}n_j - 2N\sigma_j\delta_{ij} + 2(n_j\sigma_j)\sigma_\ell\delta_{i\ell} \\ &= 2\delta_{ij}n_j - 2N\sigma_j\delta_{ij} + 2n_j\sigma_j\sigma_i, \end{aligned}$$

where $\frac{dn_i}{dn_j} = \delta_{ij}$ has been evaluated. Then, we can isolate the term with N to the LHS, getting

$$\begin{aligned} N\sigma_i &= \delta_{ij}n_j + n_j\sigma_j\sigma_i \\ &= (\delta_{ij} + \sigma_j\sigma_i)n_j. \end{aligned} \tag{3.4}$$

Since σ_i represents a vector full of ones on its entries, $N\sigma_i$ will represent a vector with N on each entry. Also, it can be noticed that $\sigma_i\sigma_j$ will represents a $(k-1)\times(k-1)$ matrix whose entries are all equal to 1, so, equation (3.4) can be interpreted as the following matricial expression

$$k-1\left\{\overbrace{\begin{bmatrix} 2 & 1 & 1 & & & \\ 1 & 2 & 1 & & \mathbf{1} & \\ 1 & 1 & 2 & & & \\ & & & \ddots & & \\ & & & & 2 & 1 & 1 \\ & \mathbf{1} & & & 1 & 2 & 1 \\ & & & & 1 & 1 & 2 \end{bmatrix}}^{k-1}\right. \begin{bmatrix} n_1 \\ \\ \vdots \\ \\ n_{k-1} \end{bmatrix} = \begin{bmatrix} N \\ \\ \vdots \\ \\ N \end{bmatrix} \tag{3.5}$$

which describes the system of equations we foresaw we were going to have. To solve it we are going to write the system as an augmented matrix, and apply row operations on it.

As we can see on Figure 3.8, the solution for equation (3.5) is where all n_i are equal to $\frac{N}{k}$. At first this system tell us this is true for all n_i from n_1 until n_{k-1}, but,

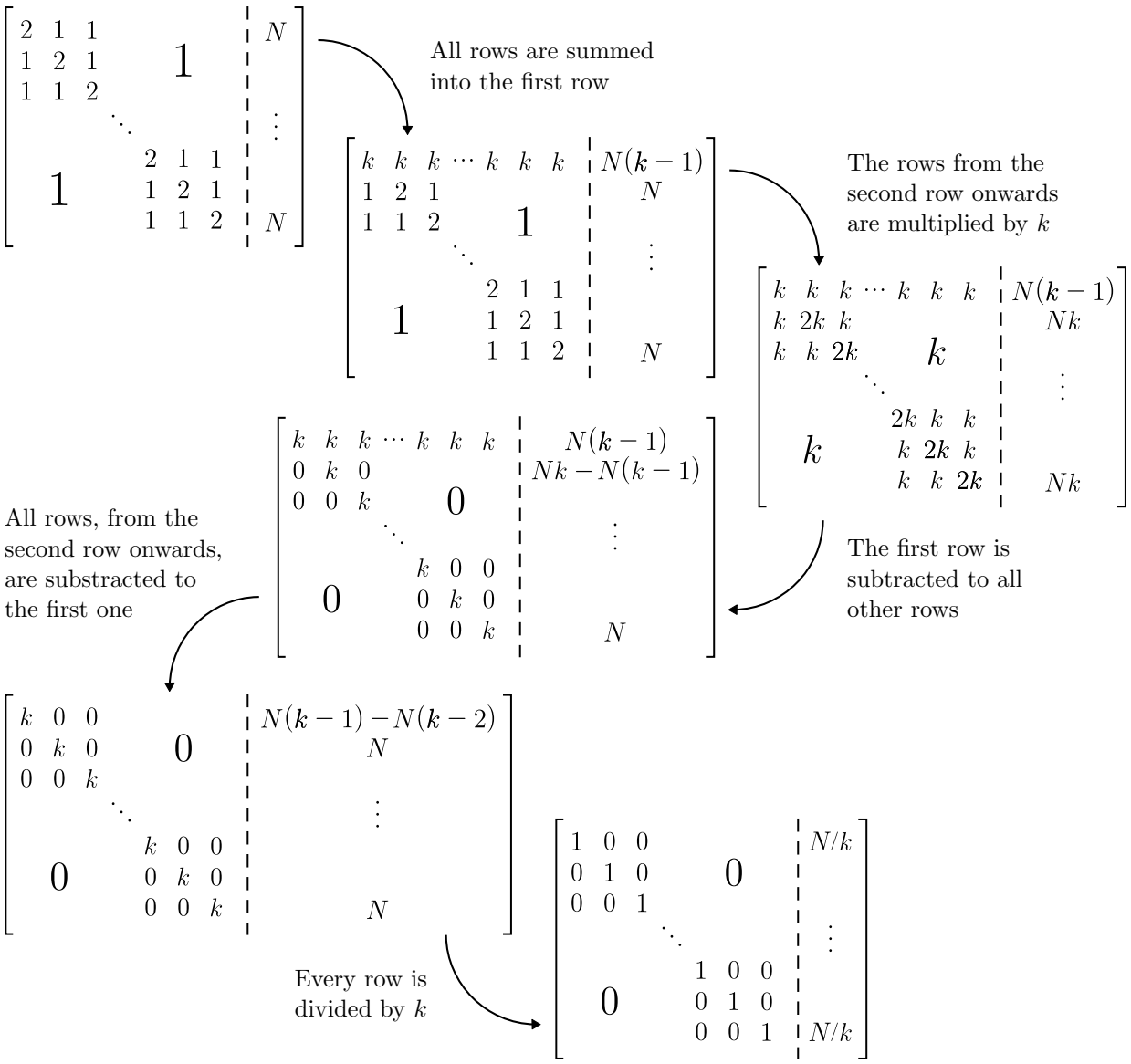

Figure 3.8: Steps for solving the system of equations of equation (3.5).

with equation (2.1) we also get that n_k is $\frac{N}{k}$. In other words

$$\min(m_\ell) = m_\ell\Big|_{\vec{n}=\left(\frac{N}{k},\ldots,\frac{N}{k}\right)}. \tag{3.6}$$

At this point someone could ask if this is really a minimum, because strictly speaking, the system we have solved so far only tell us the obtained configuration is a critical point in the configuration space. But this could also be a saddle point, or a

maximum. Well, for this, the fact that the squared matrix on equation (3.2) has its diagonal full of two's —which is positive—, means the partial derivative $\partial^2 M_\ell / \partial^2 n_i$ is going to be positive for any i, proving then this scenario is indeed a minimum of m_ℓ.

Another —much quicker, actually— way of proving this configurations posses the minimum m_ℓ value, is realizing that $\|\vec{n}\|$ is the module of the vector $\vec{n}$ on the configuration space. And due our constraint of $\sum_{i=1}^{k} n_i = N$, the minimum does not have other possibility rather than to be on the center of the space. Any leaning from that point toward any direction would increase the module of the vector, approaching to N for the extremest case. At low dimensions this is clearer to see. For instance with two vote options the minimum is at $n_i = \frac{N}{2}$ for $i \in \{1, 2\}$, as can be seen on Figure 3.9.

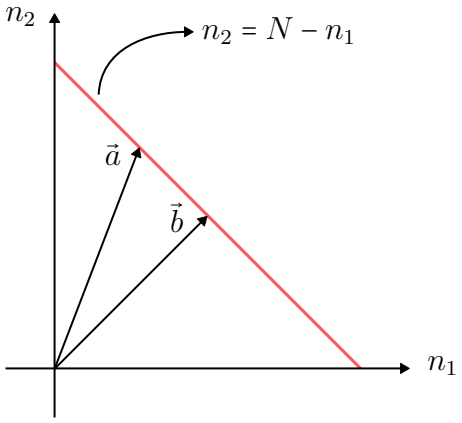

Figure 3.9: Unidimensional configuration space conformed by two vote options, described by the red line. $\vec{a}$ is a random configuration while $\vec{b} = (N/2, N/2)$.

Now, we look up for the maximum of s_ℓ. First, we are going to consider the entropy as $s_\ell = -k_B \left[p^+ \ln(p^+) + p^- \ln(p^-)\right]$ differentiate s_ℓ with respect to n_i using the chain rule as follows.

$$\frac{\partial s_\ell}{\partial n_i} = \frac{\partial s_\ell}{\partial p^+} \frac{\partial p^+}{\partial n_i}. \tag{3.7}$$

The first partial derivative is going to be

$$\frac{\partial s_\ell}{\partial p^+} = -k_B \left[(1 + \ln(p^+)) + (1 + \ln(p^-)) \left(\frac{\partial p^-}{\partial p^+} \right) \right].$$

Noting $p^- = 1 - p^+$ will give us the partial derivate of the negative-link probability with respect to the positive-link one is just -1. Then, we get

$$\frac{\partial s_\ell}{\partial p^+} = -k_B \left[(1 + \ln(p^+)) - (1 + \ln(p^-)) \right] = -k_B \left[\ln(p^+) - \ln(p^-) \right]. \tag{3.8}$$

While, the pending partial derivative is given by

$$\begin{aligned} \frac{\partial p^+}{\partial n_i} &= \frac{1}{L} \frac{\partial L^+}{\partial n_i} = \frac{1}{L} \frac{\partial}{\partial n_i} \left(\frac{1}{2} \|\vec{n}\|^2 - \frac{N}{2} \right) \\ &= \frac{\|\vec{n}\|}{L} \frac{\partial}{\partial n_i} \|\vec{n}\| \end{aligned} \tag{3.9}$$

Then, from putting equations (3.8) and (3.9) into equation (3.7), we get

$$\frac{\partial s_\ell}{\partial n_i} = -k_B \left[\ln(p^+) - \ln(p^-) \right] \left[\frac{\|\vec{n}\|}{L} \frac{\partial}{\partial n_i} \|\vec{n}\| \right] \tag{3.10}$$

If we equate equation (3.10) to zero, we will have that each of its two bracket terms could be zero. If the second is the one that becomes null, we would get that $\partial \|\vec{n}\| / \partial n_i = 0$, which we already solved from equation (3.2) to equation (3.6). It would yields us to the center of the configurations space. The first bracket, on the

other side, is zero when $L^+ = L^-$. This results on

$$\begin{aligned}
0 &= L^+ - L^- \\
&= \frac{1}{2}\left[\|\vec{n}\|^2 - N\right] - \frac{1}{2}\left[N^2 - \|\vec{n}\|^2\right] \\
&= \frac{1}{2}\left[2\|\vec{n}\|^2 - N(N+1)\right] \\
&= 2\left[\sum_{i=1}^{k-1} n_i^2 + n_k^2\right] - N(N+1) \\
&= 2\left[\sum_{i=1}^{k-1} n_i^2 + \left(N - \sum_{i=1}^{k-1} n_i\right)^2\right] - N(N+1). \qquad (3.11)
\end{aligned}$$

Then, equation (3.11) describes the configurations that are critical points of s_ℓ , aside of the center of the configuration space. Since we are interested in the case of three vote options, we evaluate $k = 3$ in the mentioned equation, getting

$$\begin{aligned}
\frac{N(N+1)}{2} &= n_1^2 + n_2^2 + (N - n_1 - n_2)^2 \\
&= N^2 + (n_1 + n_2)^2 - 2N(n_1 + n_2) + n_1^2 + n_2^2.
\end{aligned}$$

which yield us

$$\frac{N\,(N-1)}{4} = N\,(n_1 + n_2) - n_1^2 - n_1 n_2 - n_2^2. \qquad (3.12)$$

This is plotted in Figure 3.10, where can be seen how these configurations form an elipse while viewing the configuration space from above. Clearly, these would look as a circle if they were looked from a tridimensional perspective, as the previous configuration space figures. This is consistent with what can be observed on Figure 3.4, where the high entropy zone presents small depression right in the center of the configuration space.

We found this quite interesting because from the principle of maximum entropy we could lean to think that at some point there may be a tendency of the system toward these specific configurations, which are —at first glance— non trivial, far

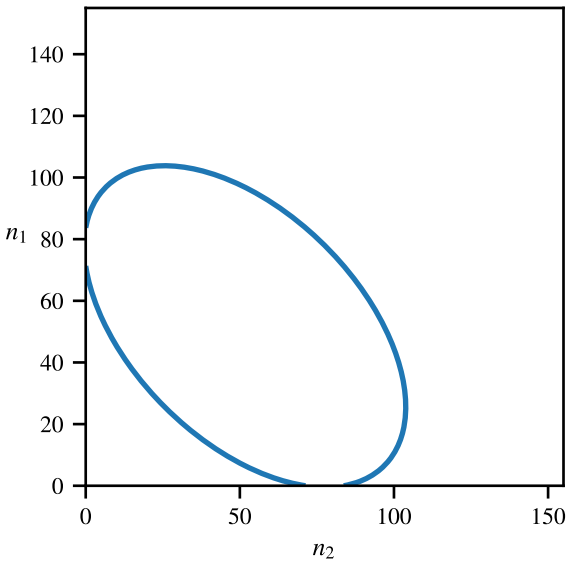

Figure 3.10: Subspace of the configuration space where link entropy is maximum. This view is from above with respect to previous plots of the configuration space, thus showing only two vote options, while the third is implicitly defined by equation (2.1).

from scenarios like unanimity or the center of the configuration space. Even though, the regions of the configuration space when a vote is disputed by two options in similar amounts is more closer to the described path on Figure 3.10. In fact, it seems the curve touches the axes around $\frac{N}{2}$.

Relationship between magnetizations and entropies

In respect to magnetizations and entropies we plot the relation between s_ℓ and m_ℓ on Figure 3.11 while in Figure 3.12 we show s_t versus m_t. On them, continuous orange lines are plotted representing equations (2.32) and (2.33), but normalized by L and C, as in equation (2.34), respectively. Also, blue dots on top of the orange lines represent possible configurations for $N = 155$.

As both equations (2.32) and (2.33) have the same structure, varying only on the magnetization that acts as independent variable, it is expected that both Figures 3.11

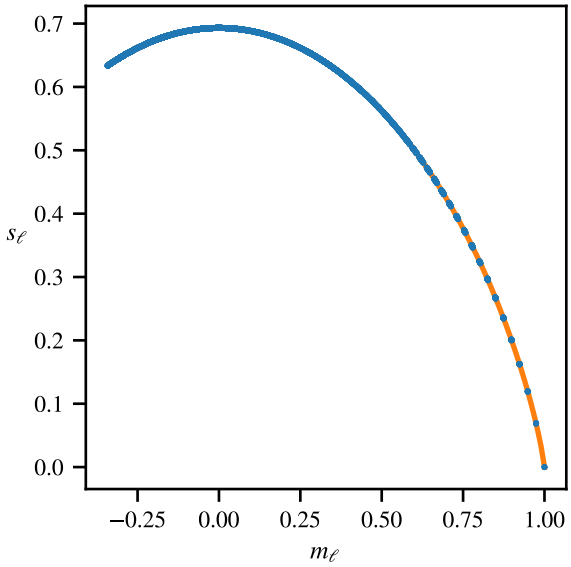

Figure 3.11: Link entropy against link magnetization. Orange line is s_ℓ from equation (2.34) while blue dots represent configurations from Figure 3.1

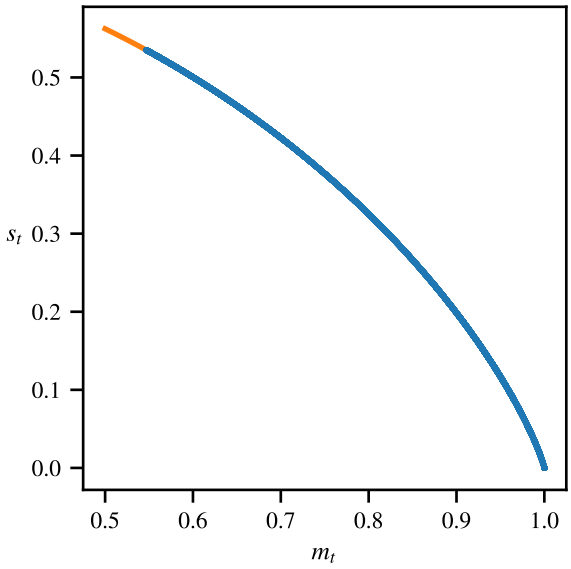

Figure 3.12: Triangle entropy against triangle magnetization. Orange line is s_t from equation (2.34) while blue dots represent configurations from Figure 3.1

and 3.12 behave the same. However, in these figures we do appreciate how both kind of magnetization do differ in domain. We know that the maximum of m_ℓ is 1, while

its minimum is defined by equation (3.6), which is

$$\min m_\ell = \frac{N}{2k}\left[N(2-k)-k\right]. \tag{3.13}$$

On the other side, triangle magnetization also has a maximum value of 1, and its minimum is on equation (2.14) at $(\frac{N}{k},\ldots,\frac{N}{k})$ as well. This give us

$$\min m_t = \frac{N}{6}\left[2-2N^2(2/k+3)-N(3+N)\right]. \tag{3.14}$$

Relation between m_ℓ and m_t

Following, we are going to dive into the relationship between the two magnetizations we have constructed. Since we do not have an analytical relation for this, on Figure 3.13 we show the relation between them from the magnetization values for the configuration space with $k = 3$ and $N = 155$. On the figure we appreciate a collection of straight lines that vary their slope and behave as an envelope of a curve similar to a parabola.

In an attempt of finding an analytical expression for this relation, we first try to parametrize the paths between the marked position. We have drawn the paths in Figure 3.14 for picture them better. Now we are going to parametrize the paths as follows, speaking in terms of part of the configuration space triangle. We encourage the reader to check Figure 3.14 to identify the path without problems.

- *From the center to a corner.* We start on the point $(\frac{N}{3},\frac{N}{3},\frac{N}{3})$. We have to borrow a node from two groups, and give them to the third. Then, the path is described by

$$A(t) = \left(\frac{N}{3}-t,\frac{N}{3}-t,\frac{N}{3}+t\right), \tag{3.15}$$

  with t for us to move across the path.

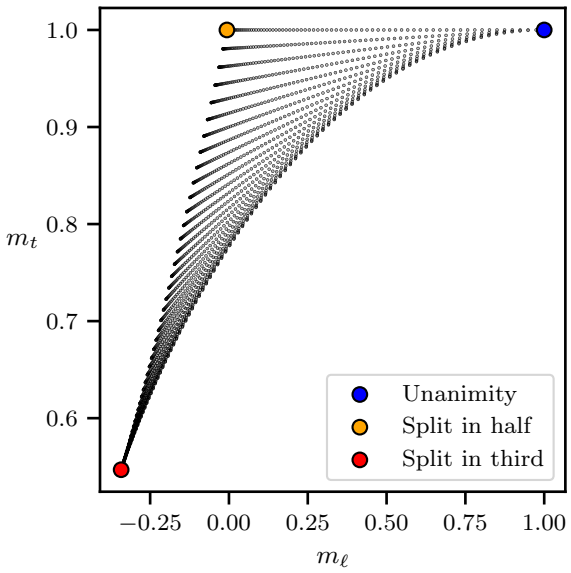

Figure 3.13: Triangle magnetization with respect to link magnetization. We have used the same label style for the relevant vote scenarios as in Figure 3.1, to illustrate the map between the configuration space and the $m_t - m_\ell$ space. Values were computed for $N = 155$.

- *From the center to the middle of a side.* We also start on the same point as before, but now we borrow two nodes from an option, and the give one to each of them two the remaining options. Then, the path is described by

$$B(t) = \left(\frac{N}{3} - 2t, \frac{N}{3} + t, \frac{N}{3} + t\right). \tag{3.16}$$

- *From the middle of a side to a corner.* We now start on the middle of a side, which we are going to note as $(0, \frac{N}{2}, \frac{N}{2})$. Now we just to borrow one node from one of the two competing options, and the give the other. Then, the path is described by

$$C(t) = \left(0, \frac{N}{2} - t, \frac{N}{2} + t\right). \tag{3.17}$$

- *Path parallel to C.* In an attempt to express the path C in a more general fashion, we define D similarly, but depending also on a new parameter α,

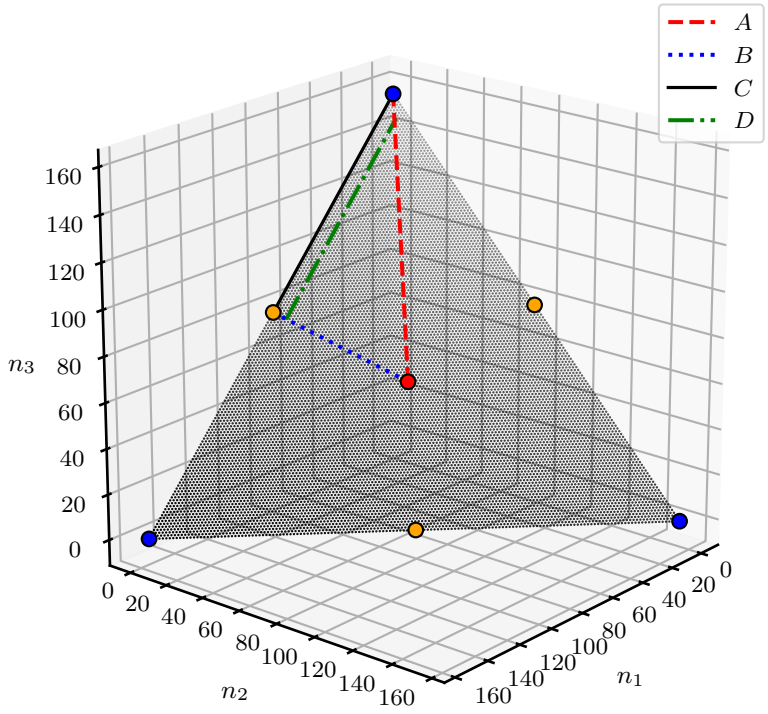

Figure 3.14: Configuration space with the same colored circles as in Figure 3.1, and with paths between these drawn. Only 1/6 of the triangle was marked up, to avoid redundancy due to the symmetry across the triangle. Paths A, B, C and D are defined in equations (3.15) to (3.18). The path D was drawn with $\alpha = 5$.

which is going to be the number of nodes the option that in C had no votes now is going to have. This number will be constant through the whole path.

$$D(t, \alpha) = \left(\alpha, \frac{N}{2} - \frac{\alpha}{2} - t, \frac{N}{2} - \frac{\alpha}{2} + t\right). \tag{3.18}$$

With these definitions for the paths we try to calculate m_ℓ and m_T values for any point on a path by evaluating the paths equations into equations (2.11) and (2.12) (and then, normalizing by L or T, accordingly). For each path we obtained the following expressions for m_ℓ and m_t, in terms of the parameter t (and α for D):

- Path A:

$$\begin{aligned} m_\ell &= \frac{-N^2 - N + \frac{2(N-3t)^2}{3}}{N(N-1)}, \\ m_t &= \frac{-N^3 - N\left(3N - 2\left(N-3t\right)^2\right) + 2N - \frac{4(N-3t)^3}{9}}{N\left(N-2\right)\left(N-1\right)}. \end{aligned} \tag{3.19}$$

- Path B:

$$\begin{aligned} m_\ell &= \frac{-\frac{N^2}{3} - N + 12t^2}{N\left(N-1\right)}, \\ m_t &= \frac{5N^3 - 27N^2 + 108Nt^2 + 18N + 216t^3}{9N\left(N^2 - 3N + 2\right)}. \end{aligned} \tag{3.20}$$

- Path C:

$$\begin{aligned} m_\ell &= \frac{-N + 4t^2}{N\left(N-1\right)}, \\ m_t &= 1. \end{aligned} \tag{3.21}$$

- Path D:

$$\begin{aligned} m_\ell &= \frac{-2N\alpha - N + 3\alpha^2 + 4t^2}{N\left(N-1\right)}, \\ m_t &= \frac{N^3 + N^2\left(-3\alpha - 3\right) + N\left(6\alpha^2 + 2\right) - 3\alpha^3 + 12\alpha t^2}{N\left(N^2 - 3N + 2\right)}. \end{aligned} \tag{3.22}$$

At this point we tried to work with these parametrical descriptions for the paths to find analytical expressions that could describe the relation we are interested in. In this process, almost none of the pairs of equations we have just presented were useful for this purpose, mainly due the complexity of the resulting mathematical expressions. Nevertheless, they were useful for plotting the paths, since —for each path— only plugging different values for t were needed. This led us to Figure 3.15 Now, the expression that were indeed useful for deriving analytical expressions were the ones of equation (3.22), which are the parametrized expression for the path D. With these two, first, we isolated the parameter t in terms of m_ℓ, and then put it in the expression for $m_t(t)$. Thus, we got that m_t in terms of m_ℓ is described by

$$m_t = \frac{3\alpha m_\ell}{N-2} + \frac{3\alpha\big[N(1-N) + 4\alpha(N-\alpha)\big]}{N(N-1)(N-2)} + 1. \tag{3.23}$$

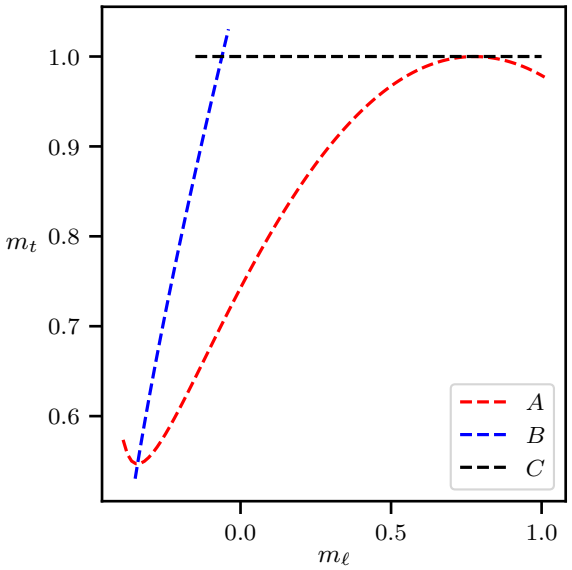

Figure 3.15: Paths A, B and C in the $m_\ell - m_t$ space. They were drawn from their parametrical descriptions on equations (3.19) to (3.21).

We can appreciate how equation (3.23) still depends on the parameter α, and will see this in fact let us distinguish between each straight line on the $m_\ell - m_t$ space. In other words, for different values of α we will expressions for different straight lines. So, these equation describes the whole family of lines in this space.

Here, on Figure 3.16, we plot the paths A, B and C as before, but now on top of the rest of points of the $m_\ell - m_t$ space. In addition, we plotted path D using equation (3.23) we just derived, with $\alpha = 5$.

Finally, we calculated an analytical expression for path A. We accomplished this taking the set of straight lines defined by equation (3.23) as the envelope for that path.

Deriving the expression for an enveloped curve takes the following steps. We differentiate the family curves equation with respect of the parameter that distinguish each curve. In this case this α. Then, we equate the resulting expression to zero and solve for the independent variable —m_ℓ in this case— in terms of the parameter (α). Finally, the main equation for the family of curves is evaluated with the obtained

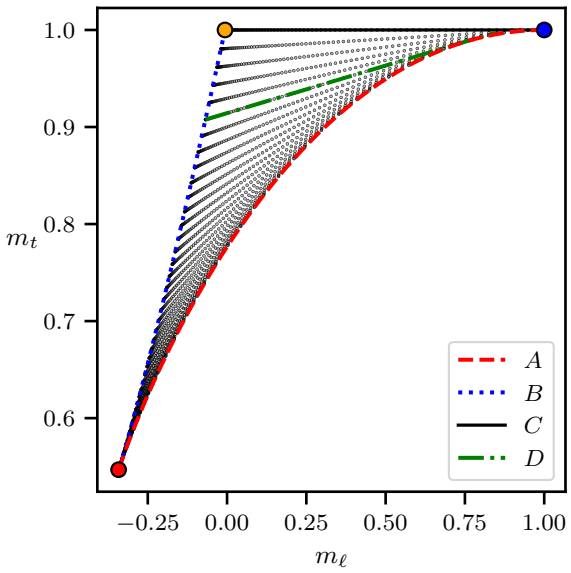

Figure 3.16: Same as in Figure 3.13, with paths A, B, C and D marked up on it. We followed the same graphic style for paths from Figure 3.14 for easier comparison. Path D was drawn with $\alpha = 5$.

expression for $\alpha(m_\ell)$ —in this case. Doing this we obtained

$$f(m_\ell) = 8N^2 - 9(N-1)(Nm_\ell - 2) - (3m_\ell(N-1) + 3 + N)^{3/2} \tag{3.24}$$

as the expression for path A. When plotted the path matches with the paths A drawn on the previous figures (actually, in Figure 3.16 path A was drawn using this equation).

3.3 Temperature

In this section we analyze the behaviour of the Temperature, which was defined in chapter 2.

Looking the analytical expressions

First, we are going to take a look into its definition on equation (2.39), given by

$$T = (N-2)\frac{2}{k_B}\left[\ln\left(\frac{1+m_\ell}{1-m_\ell}\right)\right]^{-1}.$$

Here we see the temperature may not be defined for every magnetization values. Checking where the logarithm is zero we got the temperature is undefined when $m_\ell = 0$. which is also when $L^+ = L^-$ —and when the entropy s_ℓ is maximum, recalling what we got in Section 3.2.1.

We also took the opportunity to check when the temperature is zero. For that we need the logarithm to diverge, which needs $m_\ell = 1$ or $m_\ell = -1$. Considering the minimum of m_ℓ is greater than -1, with stick with the case when $m_\ell = 1$. So, The unanimity scenario is the one with $T = 0$.

To get an idea of rest of domain for the temperature we look at Figure 3.11, where we have plotted the link entropy against the link magnetization. Since $T = \frac{\partial H}{\partial S_\ell}$ and H is proportional to m_ℓ, we know the slope on that curve will be proportional to the temperature. From the change in this slope we can anticipate we are going to have two regions. One where the temperature will be positive, and other where it will be negative.

Now we are going to look at the relation between temperature and energy. For this we have plotted equation (2.41) on Figure 3.17 with $N = 155$ and $k_B = 1$. In order to get a better picture of the behaviour of the equation we used a temperature range of $[-1e4, 1e4]$, but at this point we are yet to find if T will really fill this interval for our particular case of interest with $N = 155$.

There, a discontinuity of H is noticeable, specifically when T is zero. First, around the discontinuity H is bounded by $\frac{N}{2}(N-2)(N-1)$, as is stated on equation (2.41).

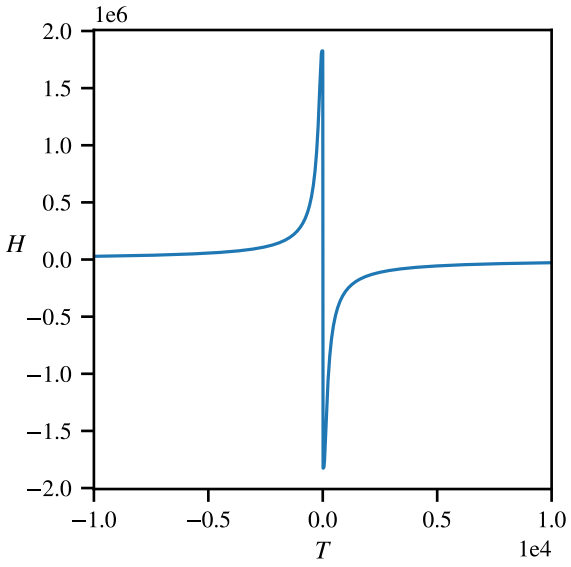

Figure 3.17: Hamiltonian against temperature, from equation (2.41) with $N = 155$ and $k_B = 1$. H is not defined of for $T = 0$, but in the plot it was considered as zero for looking purposes.

Then, if we recall —according to equation (2.41)—, for magnetization values slightly greater than zero the argument of the hyperbolic tangent goes to positive infinity and then the tangent goes to positive one. If now a slightly lesser than zero value were put into the equation, the opposite would occurs, with the tangent going to -1. Summarizing, H is undefined at $T = 0$ since crossing that point makes the energy flip its sign. The same is applicable the other way. If —for a moment— we think in the T as function of H, it also will be undefined, since over that point the temperature goes from negative infinity to positive infinity.

Temperature in the configuration space

If we plot the temperature values on the configuration space, we get the drawing of Figure 3.18. We can appreciate how the temperature values look almost entirely uniform across the plane. Also, there are noticeable points that have the greatest and lowest values of temperature. It is important to notice that the apparent uniformity

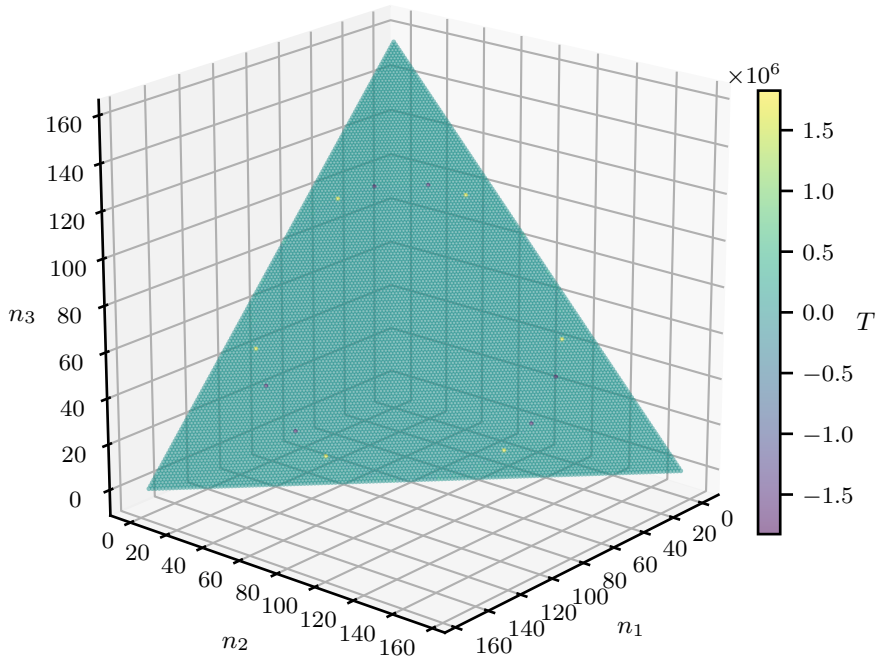

Figure 3.18: Temperature on top of the configuration space.

on the temperature values is caused by the wide range of temperature values we are coloring. Please recall for m_ℓ near to zero the temperature diverges whether toward positive or negative infinity. So, any configuration with m_ℓ close enough to zero will return us temperature values with high absolute values.

Since we still want to look how T behaves in the space that look homogeneous in Figure 3.18, we will plot the logarithm of temperature to reduce the scale. But, let us plot which parts of the configuration space have positive and negative temperature first. We do this on Figure 3.19.

The boundary between $T > 0$ and $T < 0$ looks very clear, and notice it matches the ring on Figure 3.4 with max m_ℓ, as expected. Now, we show the logarithm of temperature's absolute value on Figure 3.20. There, the ring of maximum s_ℓ is even clearer. Also, it can be seen how toward unanimity the temperature's absolute value approaches to zero.

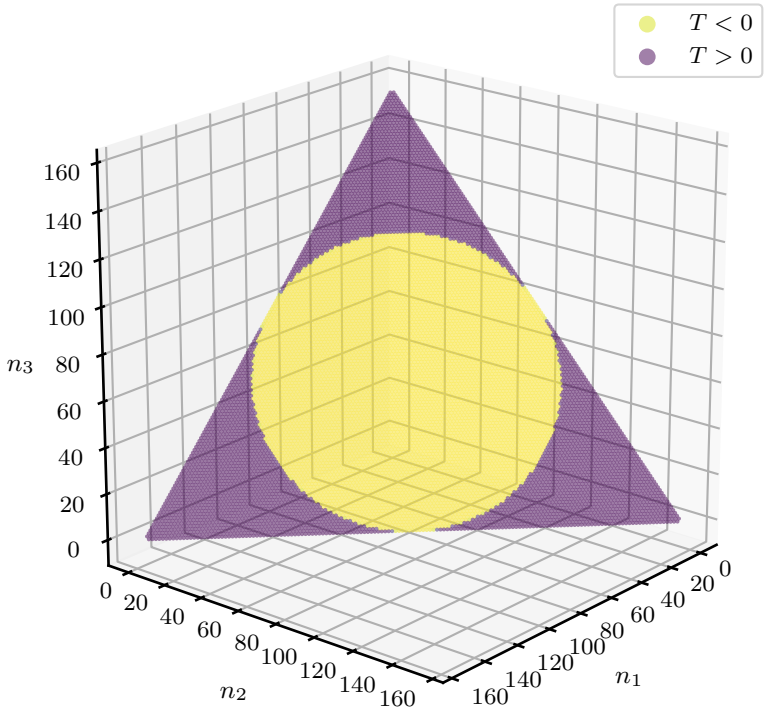

Figure 3.19: Sign of temperature on top of configuration space.

With this, we have ended our model analysis. In this chapter we focused on computing the magnetizations, the entropies and the temperature on top of the configuration space. In that process we found the link entropy does not have its maximum in the center of the configuration space, but in a ring surrounding it. We confirmed this by studying the minimum of m_ℓ and maximum of s_ℓ analytically, with consistent results. Later, we jumped into understanding the relation between m_ℓ and m_t. For that we parametrized different paths on the configuration space and mapped them into the $m_\ell - m_t$ space, and in doing that we could derive an expression that completely describe the relation between these two magnetizations.

Finally, we analyzed the defined temperature in terms of m_ℓ, and looked for posible configuration where it could be undefined or zero. Also, the dependency of the hamiltonian on temperature was studied and how the temperature is spread in the configuration space, identifying the regions where it positive and negative.

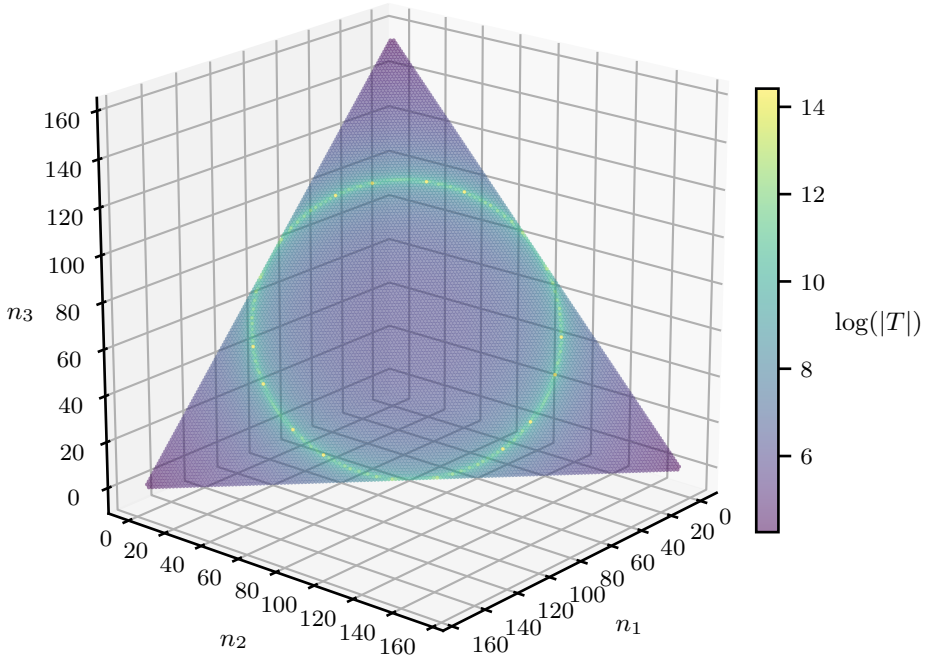

Figure 3.20: Logarithm of temperature's absolute value on top of the configuration space.

Chapter 4

Evaluation of the model with data

In this chapter we present how we evaluate some of the already presented physical magnitudes of the model with real-world data. For this we chose the Chilean Chamber of Deputies and the roll-call votes that took place on it. Specifically we will have all roll-call votes of the 2018-2022 legislative term.

4.1 About the Chilean Chamber of Deputies

In the Chilean legislative power, on each vote session, legislator can choose between three options: *for*, *against*, and *abstain*. Beside that, there are also another few situations in which a legislator can be. First of all, they can be absent. Second, the regulation let them to establish a *pareo*, in which a pair of legislators of opposite parties agree not to vote if one of them is absent at the time of voting. And finally, when there are direct conflict of interest between a legislator (or one of their relatives) and the matter at stake, their vote is said to be *dispensed*. In practice, is another way to say the person is disqualified to vote. For simplicity of the analysis, these last three situations where treated as *abstain*, to deal only with with the three main vote options.

4.2 Gathering data

The Chilean Chamber of Deputies have a transparency policy that have it make its data available for everyone. In this case, they provide an API for retrieving different type of records about their legislative activity. All the available API methods are listed on [63].

Using the `retornarVotacionesXAnno` method, we could get records listing all the votes from 2018 until 2022. From all those votes, we filtered them keeping only the ones that had occurred between March 11th of 2018 and March 10th of 2022 (beginning and end of the legislative term). This vote list also contained metadata each vote session had, which included an internal vote id, the number of *for*, *against*, and *abstain* votes, and the amount of votes that were considered as *dispensados*. These vote ids where used for calling the API method `retornarVotacionDetalle` which ask for a vote id and returns the vote roll-call detail i.e. how each present legislator voted. The data contained a list of the parlamentarias present at the time of voting, next to the option they voted.

No further filter was done to the dataset, so it contained multiple kind of votes, from each bill article approval to procedural votes of low relevance. Note we are looking for a rough quantitative analysis to evaluate our model, and, although we could have cherry-picked high relevant bills or split the records analysis by bill topics, this was not our purpose.

All the procedures mentioned in this section, from communicating with the API to retrieve the vote records, to writing the data and filtering it according to the mentioned dates, were handled with developed Python scripts.

4.3 Vote records analysis

First, we plot the vote records on top of the configuration space. On Figure 4.1 we have plot them as a red dots.

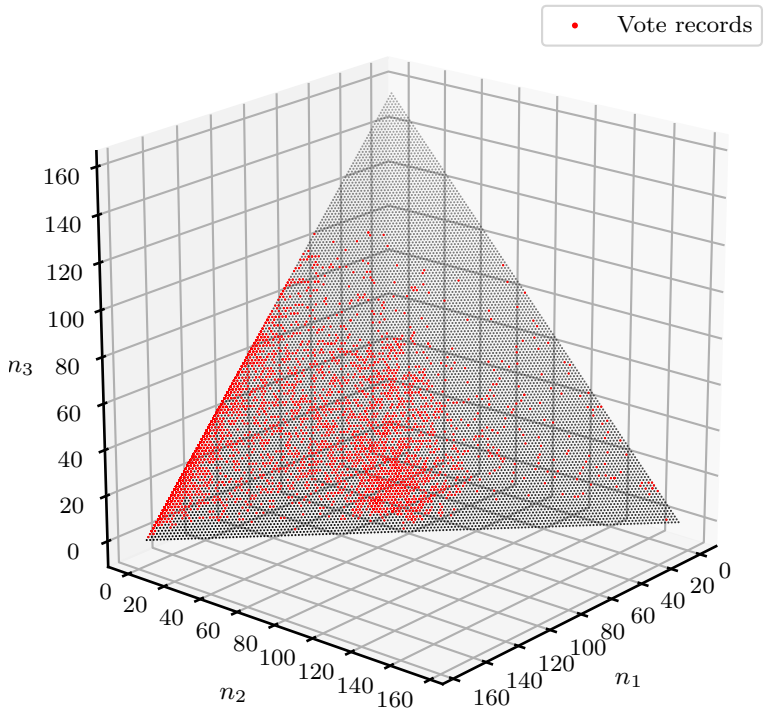

Figure 4.1: Roll-call records of the 2018-2022 term of the Chilean Chamber of Deputies, in the configuration space, represented red dots. The axes n_1, n_2 and n_3 represent the options *for*, *against*, and *abstain*, respectively.

Analyzing the data we found that the part of the phase space with more points is around the lower half of the left edge of the phase-space triangle, which indeed looks like a thick stripe of dots on Figure 4.1. Now, paying attention on the axes, this tells us votes are mainly in dispute between *for* and *abstain* options. This do not necessarily says that there are more real-*abstain* votes than *against* ones, because we must recall our assumptions for *abstention* also included the absence (where most high *abstain* values might come from) and the situations of *pareos* and *dispensed* votes (which should conform just a tiny part of *abstain* votes, since these occur at small scale).

We also computed the mean position of the roll-call records and plot it on Figure 4.2. There we included the region where $L^+ = L^-$ to show that, although this point its not in that region it is very close. Moreover, we calculate basic statistics

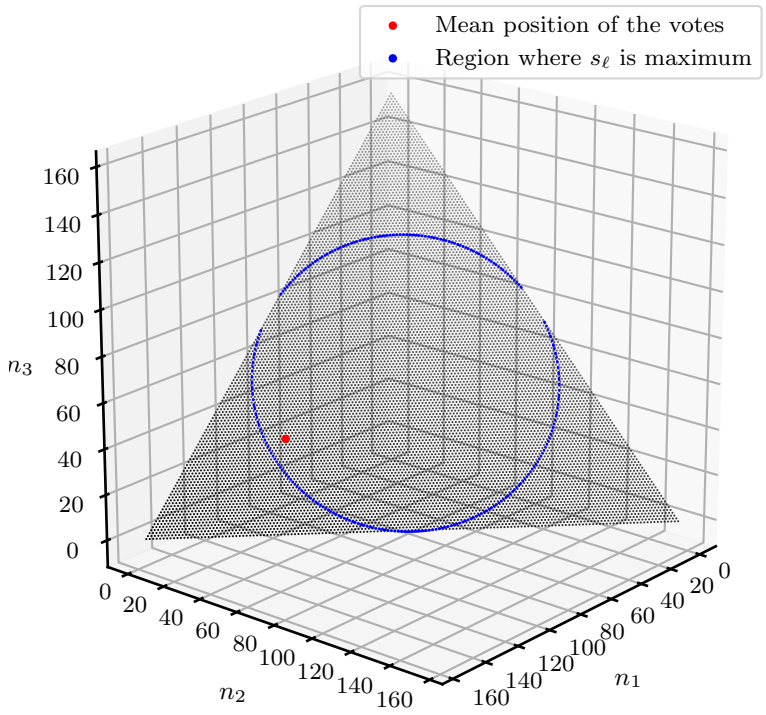

Figure 4.2: Configuration space with the mean position of roll-call records of the 2018-2022 term of the Chilean Chamber of Deputies, painted as a red dot on top of it. In addition the ring of maximum s_ℓ was drawn for reference. The axes n_1, n_2 and n_3 represent the same as in Figure 4.1.

for the physical properties of the dataset and show them on Table 4.1. It can be seen that average values for this quantities may not represent the dataset the best due the high values for the standard deviations, specially the ones that are bigger than the absolute value of their associated mean, like for m_ℓ, H and T.

Finally, in the following figures (Figures 4.3 and 4.5 to 4.7) we show the fluctuations of these quantities. In these the horizontal axis represent the vote number, starting with 0. Since the frequency of votes it is not constant, drawing the votes in chronological order is got-to way of plotting them across a temporal-like dimension.

Table 4.1: Statistical measure for the physical properties of the vote records.

	Mean	Standard deviation
m_ℓ	0.116	0.343
m_t	0.855	0.154
s_ℓ	0.622	0.099
s_t	0.210	0.199
H	6.028e2	4.571e4
T	−2.125e5	6.266e5

Also, in all of them we have plot the raw series on the top panel, while in the lower panel we have plotted the series taking the average value for windows of 50 points. In addition we have marked the average of each plot as a red line.

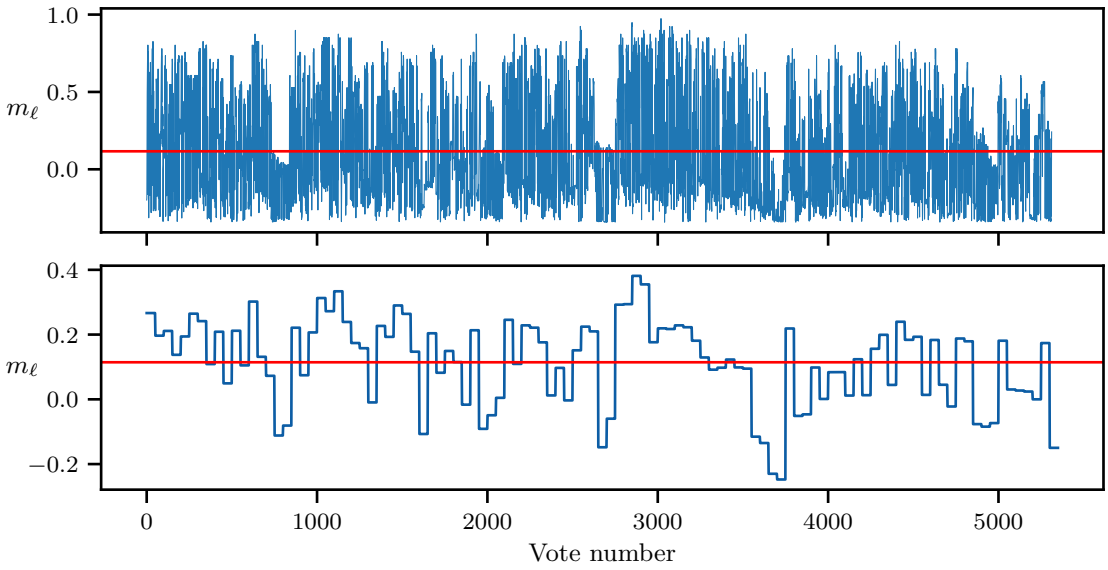

Figure 4.3: Fluctuation of the link magnetization. Top panel: raw series; lower panel: average every 50 consecutive data points. Red lines represent the mean value for each plot.

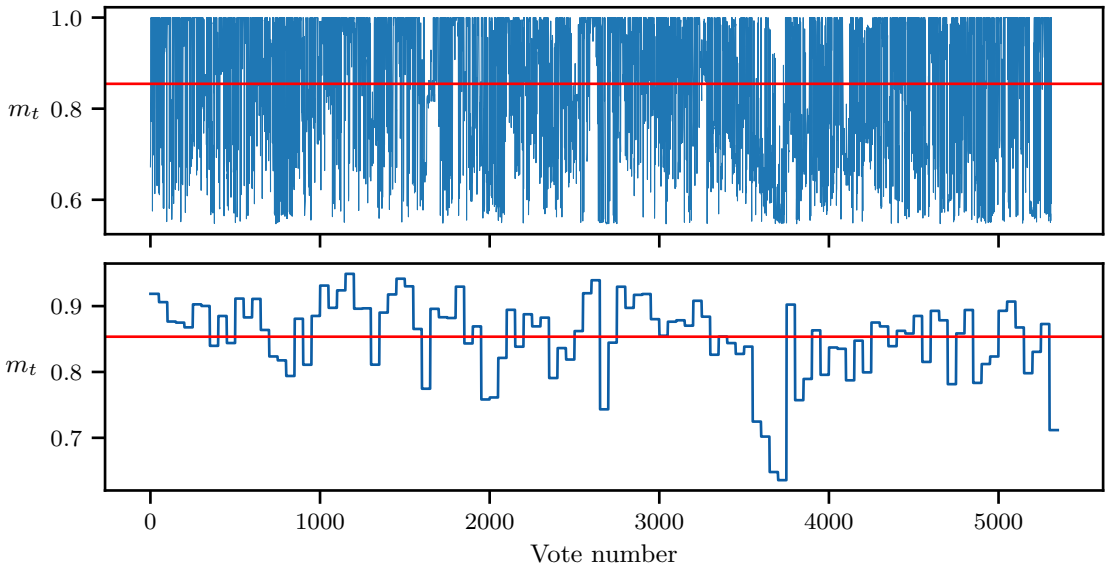

Figure 4.4: Fluctuation of the triangle magnetization. Top panel: raw series; lower panel: average every 50 consecutive data points. Red lines represent the mean value for each plot.

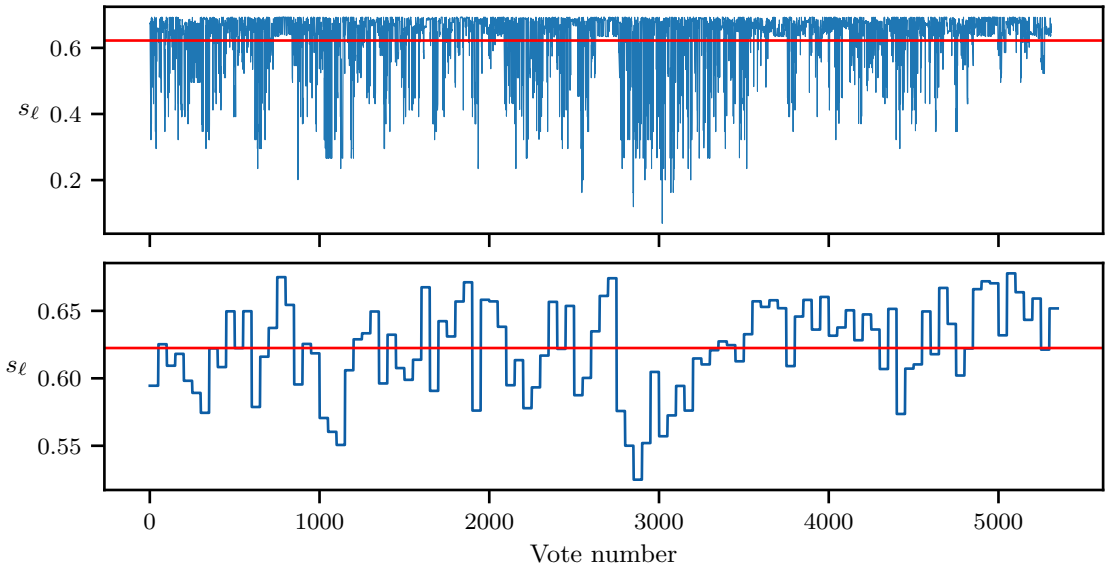

Figure 4.5: Fluctuation of the link entropy (computed with $k_B = 1$). Top panel: raw series; lower panel: average every 50 consecutive data points. Red lines represent the mean value for each plot.

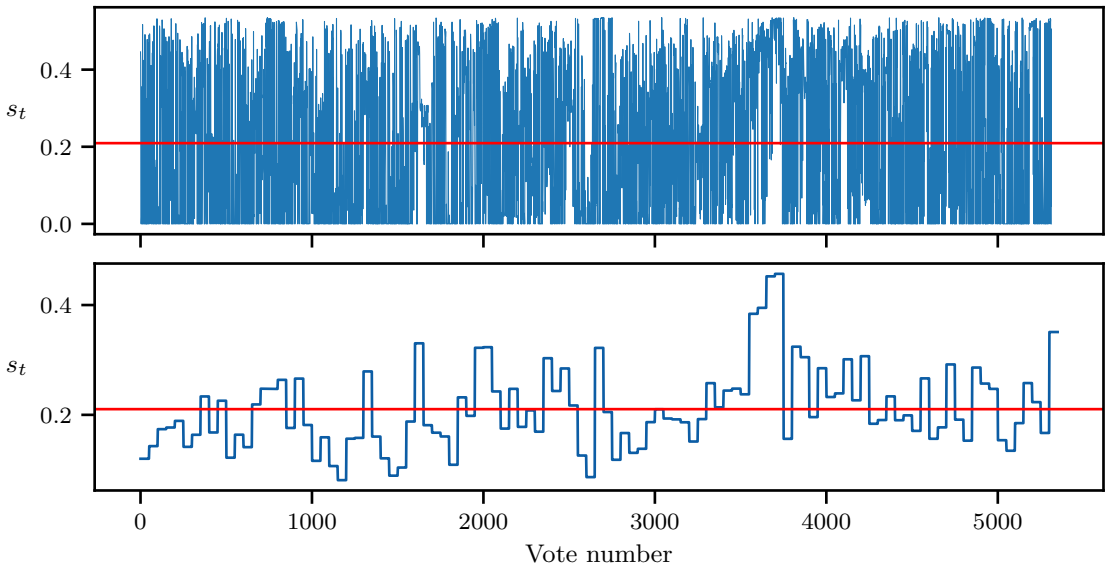

Figure 4.6: Fluctuation of the triangle magnetization (computed with $k_B = 1$). Top panel: raw series; lower panel: average every 50 consecutive data points. Red lines represent the mean value for each plot.

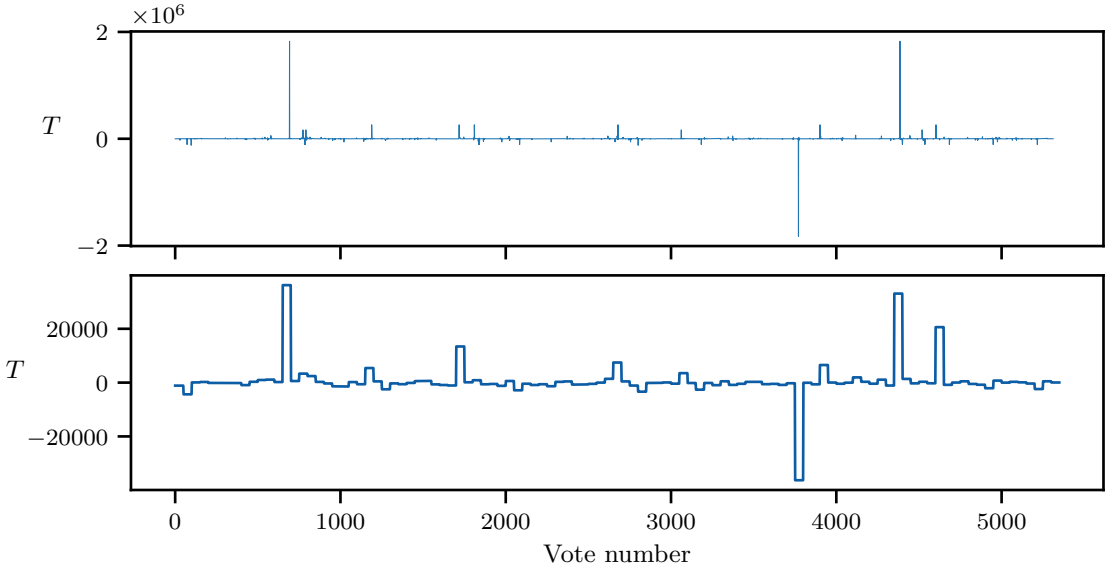

Figure 4.7: Fluctuation of the T (computed with $k_B = 1$). Top panel: raw series; lower panel: average every 50 consecutive data points. Red lines represent the mean value for each plot.

Chapter 5

Discussion and conclusions

In this last chapter we are going to review the major insights that we got from the presented work, and their implications.

5.1 About related work

We want to compare our model with the one that has been presented on Belaza *et al.* [64]. This work is the most similar to ours we could find, so we considered important to discuss the similarities and differences. In that article Belaza *et al.* also present a statistical mechanics model for balance theory with focus on political networks. A clear similarity come from the Hamiltoninan they proposed, which is

$$H = \sum_{i<j<k} \left[\underbrace{-\alpha s_{ij}s_{jk}s_{ki}}_{\text{three-body}} \underbrace{-\gamma\left(s_{ij}s_{jk} + s_{ij}s_{ki} + s_{jk}s_{ki}\right)}_{\text{two-body}} \underbrace{+\omega\left(s_{ij} + s_{jk} + s_{ki}\right)}_{\text{one-body}} \right],$$

with s_{ij} being 1 or -1 if there were a link between nodes i and j with that sign, or 0 otherwise; also, the sum indexes $i < j < k$ go through every single triad of nodes. Here, we can note that the "one-body" term coincides with the definition of our Hamiltonian (leaving the ω factor aside). That term is summing the sides of

each triangle, so basically is the same we showed on Section 2.4. Also, the "three-body" term is summing each triangle balances, so at the end it would be something proportional to M_t.

Despite that, the general structure of the work is pretty different than our. They assume a random network where all four types of triangles are possible with addition of the possibility that may be triads of nodes that end up not begin connected, this marking a huge difference between the approaches. Instead we start from a fully connected network —throwing out the situation of a triad not being connected— and our criteria for assigning positive or negative sign to the links make impossible to have the triangle of type $[+ + -]$.

Another big difference was the chosen ensamble to work in. The developed model in this thesis took the microcanonical ensamble as a framework. This choice is justified by the fact we wanted to assume that each microstate would have the same probability and to have a constant energy. Also we were looking to derive the temperature for the system rather than taking it as an external parameter for the system. On the other side, [64] used the canonical ensamble, which gave probabilities for each configuration of the system in terms of the temperature. We did not derived probabilities that could tell us which vote scenario is more probable than the rest, but we think this might be possible if we extend our formalism toward a canonical formulation. In that scenario, we think the configuration space we presented —for the microcanonical ensamble— would turn into a phase space —for the canonical ensamble.

5.2 About strong polarization

As we mentioned in Section 1.3, this work was motivated by the work present on Neal [43] where *strong polarization* is introduced. There, the author stated this new type of polarization could be quantified via the triangle-index, which is defined as the proportion of balanced triangles between the total number of triangles. We note this metric is equal to the probability of finding a balanced triangle among all triangles, which we have noted as p_t^+ in Section 3.2. If we recall equation (2.30), we would note that it has a direct relation with the triangle magnetization (m_t). Nevertheless, high m_t does not imply high *strong polarization*.

We have to remember that [43] considered multiple bill's data for building the network, so we can not hang on exactly the same interpretation of that metric. Since our model took relations between legislators from a single vote session during its formulation, it may not be appropriate to talk about *polarization* as such while evaluating it with particular vote configurations. A political system is not going to be polarized by just one vote session, but the outcomes of multiple votes through time may indeed be an indicator if a parliament has been more polarized or not. Following the same line, a single value of energy or temperature for a given vote outcome it is not going to tell us much more about a system, but we think a collection of physical properties for a large dataset of roll-call vote records will do. However, we recognized the presented work does not aboard this.

The model we have presented offers a physical formalism to quantify disagreement from roll-call votes outcomes. This goes in the direction of understanding what *strong polarization*, but by itself it is not enough. In order to accomplish it, we think an analysis for the physical properties $(m_\ell, m_t, s_\ell, s_t, H, T)$ of a set of multiple votes might be needed. For this, comparing the model with a larger dataset could be useful, and extending the formalising toward a canonical ensamble may help as well.

5.3 About the physical magnitudes

Magnetizations and energy

In the analysis of the model we showed the magnetizations on top of the configuration space, specifically on Figures 3.2 and 3.3. From there we notice m_ℓ has its maximum values toward the corners of the configuration space triangles. In some extent, this is expected. Due the way we assign the link signs in the network, toward the unanimity configurations we will have mostly positive links, so the magnetization tends to 1. Then we could say m_ℓ represent how close or far a vote is from unanimity.

The behaviour for m_t —the subtraction of balanced triangles minus the unbalanced ones— is a bit different. Seems it can not distinguish between a unanimous vote and a vote disputed between two options. This is can be explained recalling the only unbalanced triangles in our network are of type $[---]$ and that with two vote option we are not going to have those. Around legislators that vote different there are only going to be $[+--]$ triangles, which are balanced. Thus m_t will be an indicator of how much close a vote is of having at least one option without votes, with its value being equal to 1 when at leas one option already have no support.

Regarding the energy, we clarify we did not plotted the Hamiltonian on Section 3.2 because —since is proportional to the link magnetization —all that can be inferred from the m_ℓ plot is equivalent for the energy (but with opposite sign due the negative sign on equation (2.20)). Then, its meaning would be the same as m_ℓ i.e. how much far from unanimity a vote is. And actually, if we remember, in Section 2.4 we choose the Hamiltonian looking its minimization would occur for the unanimity scenario, so in some way this is expected.

Potential works could be testing this thesis's model with a different Hamiltonian or modifying the current one, adding new terms to it similarly as in [64]. This may be

helpful if we wanted to give more relevance to m_t or to triangles balance in general. In that scenario relations between magnetizations we have derived on Section 3.2.3 could be essential for linking potential analysis with the one we presented in this thesis.

Entropies

For the entropies we can hang on the interpretation for entropy as a measure of "surprise" or uncertainty for a given configuration. For example we notice s_ℓ has its minimum on the corners of the configuration space triangle. In those unanimous cases we know there will be positive links only, if we were picking a random link from the network there would be no doubt that it would be positive. Thus, zero entropy. Again, if we moved away from the corner we would note a growth on the entropy.

As we mentioned earlier, the maximum of s_ℓ surround the center of the configuration space in a region described by $L^+ = L^-$. So, in this case we have fifty percent chance of drawing a positive or negative link from the network, then this the most uncertain situation.

Regarding this entropy, in Chapter 4 we showed that the average position for votes of the Chilean Chamber Deputies in the configuration space was close the region with maximum s_ℓ. This may suggest that the system —in average— actually tends toward these configurations. Nevertheless, the used dataset may be not large enough to be statistically representative. Records of votes from multiple legislative terms may help to test this.

The triangle entropy on the other side, does not express much more than the triangle magnetization. The behaviour is practically analogous but upside-down. We could think this as the uncertainty of having at least one option without votes. On the sides, as we mentioned above, we know for sure one option has no support. Thus, zero entropy. Then, the closer to the center the higher the entropy.

Finally, about the variant triangle entropy $\tilde{s}_t$ on Figure 3.7 it can be seen that it has three maximums. Despite we did not analyze the behaviour of this quantity, we guess these could be where $C_{+++} = C_{+--} = C_{---}$ so the uncertainty is maximum. Due this entropy does not have a magnetization counterpart, a more detained on it was left for future works.

Temperature

The temperature resulted in a quantity that may summarize what the other physical magnitudes tell us. This is equal to zero at *unanimity* and from there toward the center the configuration space starts growing, but the closer to the region $L^+ = L^-$ a vote gets the higher the temperature, diverging exactly in this boundary. All this can be observed in Figures 3.18 and 3.20. Crossing it the temperature presents negative values, meaning there there is high energy but no much entropy. This region ($T < 0$) also represent where the energy is negative, meaning there are more negative than positive relations in the network.

What happens on that boundary can also be studied analyzing the divergence on the $H - T$ plot of Figure 3.17. There we may notice that looking the picture the other way —like temperature in function of energy—, passing from positive to negative energy, the temperature flips from minus infinity to positive infinity, being this discontinuity on the temperature another way to interpret the maximum link entropy.

5.4 Final conclusions

Looking for a physical way to describe *strong polarization* [43] we constructed a statistical mechanics model for a specific case of legislative networks from roll-call

votes, choosing the sign for the links between legislators according the agreement (or not) in the options they voted. Although at first our idea was to focus on the triangles and their balance, we recognize most of our analysis ended up being more about the links and about the link magnetization and entropy, where we found interesting phenomena.

Part of this is caused by the fact our Hamiltonian ended up depending on the link magnetization only, but in the larger picture —we think— this was highly influenced by the way we build our network and how we assigned the link signs. For example, this also caused the triangle-index to lose its interpretation from [43], so it got harder to keep track of what *strong polarization* was.

Despite that, we can say we were able to successfully build a model where links and triangles in the network were treated as spins. There, spins states were given by the sign or the balance of links and triangles, and therefrom we derived different physical magnitudes such as magnetizations, entropies and temperature. All this was done analytically considering an arbitrary amount of options k, although later we fixed this to 3 on some calculations for simplification purposes. This last based on that most commonly vote have three options: *for*, *against*, and *abstain*.

Finally, the model we have presented offers a physical formalism to quantify disagreement from roll-call votes outcomes, and although it cannot told us about polarization yet, goes in that direction, paving the way for potential works that may extend it.

Bibliography

1. Castellano, C., Fortunato, S. & Loreto, V. Statistical Physics of Social Dynamics. *Reviews of Modern Physics* **81,** 591–646. doi:10.1103/revmodphys.81.591 (May 11, 2009).

2. Weidlich, W. The Statistical Description of Polarization Phenomena in Society†. *British Journal of Mathematical and Statistical Psychology* **24,** 251–266. doi:10.1111/j.2044-8317.1971.tb00470.x (1971).

3. Galam, S., Gefen (Feigenblat), Y. & Shapir, Y. Sociophysics: A New Approach of Sociological Collective Behaviour. I. Mean-behaviour Description of a Strike. *The Journal of Mathematical Sociology* **9,** 1–13. doi:10.1080/0022250X.1982.9989929 (Nov. 1, 1982).

4. Galam, S. Application of Statistical Physics to Politics. *Physica A: Statistical Mechanics and its Applications* **274,** 132–139. doi:10.1016/S0378-4371(99)00320-9 (Dec. 1, 1999).

5. Galam, S. Real Space Renormalization Group and Totalitarian Paradox of Majority Rule Voting. *Physica A: Statistical Mechanics and its Applications* **285,** 66–76. doi:10.1016/S0378-4371(00)00272-7 (Sept. 2000).

6. Stauffer, D., Sousa, A. O. & De Oliveira, S. M. Generalization to Square Lattice of Sznajd Sociophysics Model. *International Journal of Modern Physics C* **11,** 1239–1245. doi:10.1142/S012918310000105X (Sept. 2000).

7. Stauffer, D. Sociophysics: The Sznajd Model and Its Applications. *Computer Physics Communications. Proceedings of the STATPHYS Satellite Conference: Challenges in Computational Statistical Physics in Teh 21st Century* **146,** 93–98. doi:10.1016/S0010-4655(02)00439-3 (June 15, 2002).

8. Suchecki, K., Eguíluz, V. M. & Miguel, M. S. Conservation Laws for the Voter Model in Complex Networks. *Europhysics Letters (EPL)* **69,** 228–234. doi:10.1209/epl/i2004-10329-8 (Jan. 2005).

9. Axelrod, R. The Dissemination of Culture: A Model with Local Convergence and Global Polarization. *Journal of Conflict Resolution* **41,** 203–226. doi:10.1177/0022002797041002001 (Apr. 1, 1997).

10. Castellano, C., Marsili, M. & Vespignani, A. Nonequilibrium Phase Transition in a Model for Social Influence. *Physical Review Letters* **85,** 3536–3539. doi:10.1103/PhysRevLett.85.3536 (Oct. 16, 2000).

11. Wichmann, S. The Emerging Field of Language Dynamics. *Language and Linguistics Compass* **2,** 442–455. doi:10.1111/j.1749-818X.2008.00062.x (2008).

12. Keller, M., Festinger, L., Schachter, S. & Back, K. Social Pressures in Informal Groups, a Study of Human Factors in Housing. *The Milbank Memorial Fund Quarterly* **30,** 384. doi:10.2307/3348388 (1950).

13. Euler, L. Solutio Problematis Ad Geometriam Situs Pertinentis. *Commentarii academiae scientiarum Petropolitanae,* 128–140. https://scholarlycommons.pacific.edu/euler-works/53 (Jan. 1, 1741).

14. Vecchio, F., Miraglia, F. & Maria Rossini, P. Connectome: Graph Theory Application in Functional Brain Network Architecture. *Clinical Neurophysiology Practice* **2,** 206–213. doi:10.1016/j.cnp.2017.09.003 (Jan. 1, 2017).

15. Urban, D. & Keitt, T. Landscape Connectivity: A Graph-Theoretic Perspective. *Ecology* **82,** 1205–1218. doi:10.1890/0012-9658(2001)082[1205:LCAGTP]2.0.CO;2 (2001).

16. Keeling, M. J. & Eames, K. T. Networks and Epidemic Models. *Journal of The Royal Society Interface* **2,** 295–307. doi:10.1098/rsif.2005.0051 (June 20, 2005).

17. Tapiero, C. S. The Theory of Graphs in Behavioral Science*. *Decision Sciences* **3,** 57–81. doi:10.1111/j.1540-5915.1972.tb00526.x (1972).

18. Castro, N. & Siew, C. S. Q. Contributions of Modern Network Science to the Cognitive Sciences: Revisiting Research Spirals of Representation and Process. *Proceedings of the Royal Society A: Mathematical, Physical and Engineering Sciences* **476,** 20190825. doi:10.1098/rspa.2019.0825 (June 10, 2020).

19. Maas, C. Computing and Interpreting the Adjacency Spectrum of Traffic Networks. *Journal of Computational and Applied Mathematics* **12–13,** 459–466. doi:10.1016/0377-0427(85)90039-1 (May 1, 1985).

20. Maćkiewicz, A. & Ratajczak, W. Towards a New Definition of Topological Accessibility. *Transportation Research Part B: Methodological* **30,** 47–79. doi:10.1016/0191-2615(95)00020-8 (Feb. 1, 1996).

21. Strohmaier, M. & Wagner, C. Computational Social Science for the World Wide Web. *IEEE Intelligent Systems* **29,** 84–88. doi:10.1109/MIS.2014.80 (Sept. 2014).

22. Majeed, A. & Rauf, I. Graph Theory: A Comprehensive Survey about Graph Theory Applications in Computer Science and Social Networks. *Inventions* **5,** 10. doi:10.3390/inventions5010010 (1 Mar. 2020).

23. Watts, D. J. & Strogatz, S. H. Collective Dynamics of 'Small-World' Networks. *Nature* **393,** 440–442. doi:10.1038/30918 (6684 June 1998).

24. Barabási, A.-L. & Albert, R. Emergence of Scaling in Random Networks. *Science* **286,** 509–512. doi:10.1126/science.286.5439.509 (Oct. 15, 1999).

25. Newman, M. & Girvan, M. Finding and Evaluating Community Structure in Networks. *Physical Review E* **69,** 026113–026113. doi:10.1103/physreve.69.026113 (Feb. 26, 2004).

26. Newman, M. Fast Algorithm for Detecting Community Structure in Networks. *Physical Review E* **69,** 066133–066133. doi:10.1103/physreve.69.066133 (June 18, 2004).

27. Newman, M. Modularity and Community Structure in Networks. *Proceedings of the National Academy of Sciences of the United States of America* **103,** 8577–8582. doi:10.1073/pnas.0601602103 (June 6, 2006).

28. Newman, M. The Structure and Function of Complex Networks. *Siam Review* **45,** 167–256. doi:10.1137/s003614450342480 (Jan. 1, 2003).

29. Cantwell, G. T., Kirkley, A. & Newman, M. E. J. The Friendship Paradox in Real and Model Networks. *Journal of Complex Networks* **9** (ed Estrada, E.) cnab011. doi:10.1093/comnet/cnab011 (May 5, 2021).

30. Da Fontoura Costa, L., Rodrigues, F. A. & Cristino, A. S. Complex Networks: The Key to Systems Biology. *Genetics and Molecular Biology* **31,** 591–601. doi:10.1590/s1415-47572008000400001 (Jan. 1, 2008).

31. Karrer, B. & Newman, M. Competing Epidemics on Complex Networks. *Physical Review E* **84,** 036106–036106. doi:10.1103/physreve.84.036106 (Sept. 9, 2011).

32. Montes-Orozco, E. *et al.* Identification of COVID-19 Spreaders Using Multiplex Networks Approach. *IEEE Access* **8,** 122874–122883. doi:10.1109/access.2020.3007726 (July 7, 2020).

33. Dods, J., Chapman, S. C. & Gjerloev, J. Network Analysis of Geomagnetic Substorms Using the SuperMAG Database of Ground-Based Magnetometer Stations. *Journal of Geophysical Research* **120,** 7774–7784. doi:10.1002/2015ja021456 (Sept. 26, 2015).

34. Erdős, P. & Rényi, A. On Random Graphs. I. *Publicationes Mathematicae Debrecen* **6,** 290–297. doi:10.5486/PMD.1959.6.3-4.12 (1959).

35. Clauset, A., Newman, M. & Moore, C. Finding Community Structure in Very Large Networks. *Physical Review E* **70,** 066111–066111. doi:10.1103/physreve.70.066111 (Dec. 6, 2004).

36. Duch, J. & Arenas, A. Community Detection in Complex Networks Using Extremal Optimization. *Physical Review E* **72,** 027104–027104. doi:10.1103/physreve.72.027104 (Aug. 24, 2005).

37. Blondel, V. D., Guillaume, J.-L., Lambiotte, R. & Lefebvre, E. Fast Unfolding of Communities in Large Networks. *Journal of Statistical Mechanics: Theory and Experiment.* doi:10.1088/1742-5468/2008/10/p10008 (Mar. 4, 2008).

38. Reichardt, J. & Bornholdt, S. Statistical Mechanics of Community Detection. *Physical Review E* **74,** 016110. doi:10.1103/physreve.74.016110 (July 18, 2006).

39. Karrer, B. & Newman, M. E. J. Stochastic Blockmodels and Community Structure in Networks. *Physical Review E* **83,** 016107. doi:10.1103/PhysRevE.83.016107 (Jan. 21, 2011).

40. Peixoto, T. P. Nonparametric Bayesian Inference of the Microcanonical Stochastic Block Model. *Physical Review E* **95,** 012317. doi:10.1103/PhysRevE.95.012317 (Jan. 17, 2017).

41. Peixoto, T. P. in *Advances in Network Clustering and Blockmodeling* 289–332 (John Wiley & Sons, Ltd, 2019). doi:10.1002/9781119483298.ch11.

42. Wasserman, S. & Faust, K. *Social Network Analysis: Methods and Applications* (Nov. 25, 1994).

43. Neal, Z. P. A Sign of the Times? Weak and Strong Polarization in the U.S. Congress, 1973–2016. *Social Networks* **60,** 103–112. doi:10.1016/j.socnet.2018.07.007 (Jan. 1, 2020).

44. Marenco, L., Carmona, H. A., Felipe Maciel Cardoso, Andrade, J. S. & Cesar, C. L. Time Evolution of the Behaviour of Brazilian Legislative Representatives Using a Complex Network Approach. *PLOS ONE* **15.** doi:10.1371/journal.pone.0226504 (Feb. 5, 2020).

45. Intal, C. & Yasseri, T. Dissent and Rebellion in the House of Commons: A Social Network Analysis of Brexit-related Divisions in the 57th Parliament. *Applied Network Science* **6,** 36. doi:10.1007/s41109-021-00379-2 (Dec. 2021).

46. Schoch, D. & Brandes, U. Legislators' Roll-Call Voting Behavior Increasingly Corresponds to Intervals in the Political Spectrum. *Scientific Reports* **10,** 17369–17369. doi:10.1038/s41598-020-74175-w (2020).

47. Alemán, E. & Calvo, E. Explaining Policy Ties in Presidential Congresses: A Network Analysis of Bill Initiation Data. *Political Studies* **61,** 356–377. doi:10.1111/j.1467-9248.2012.00964.x (June 1, 2013).

48. Zhao, X., Yang, B., Liu, X. & Chen, H. Statistical Inference for Community Detection in Signed Networks. *Physical Review E* **95,** 042313. doi:10.1103/PhysRevE.95.042313 (Apr. 17, 2017).

49. Fowler, J. H. Connecting the Congress: A Study of Cosponsorship Networks. *Political Analysis* **14,** 456–487. doi:10.1093/pan/mpl002 (Oct. 2006).

50. Fowler, J. H. Legislative Cosponsorship Networks in the US House and Senate. *Social Networks* **28,** 454–465. doi:10.1016/j.socnet.2005.11.003 (Oct. 1, 2006).

51. Porter, M. A., Mucha, P. J., Newman, M. E. J. & Warmbrand, C. M. A Network Analysis of Committees in the U.S. House of Representatives. *Proceedings of the National Academy of Sciences* **102,** 7057–7062. doi:10.1073/pnas.0500191102 (May 17, 2005).

52. Andris, C. *et al.* The Rise of Partisanship and Super-Cooperators in the U.S. House of Representatives. *PLOS ONE* **10,** e0123507. doi:10.1371/journal.pone.0123507 (Apr. 21, 2015).

53. Briatte, F. Network Patterns of Legislative Collaboration in Twenty Parliaments. *Network Science* **4,** 266–271. doi:10.1017/nws.2015.31 (June 1, 2016).

54. Le Foulon Morán, C. Cooperation and Polarization in a Presidential Congress: Policy Networks in the Chilean Lower House 2006–2017: *Politics* **40,** 227–244. doi:10.1177/0263395719862478 (May 1, 2020).

55. Zhang, Y. *et al.* Community Structure in Congressional Cosponsorship Networks. *Physica A: Statistical Mechanics and its Applications* **387,** 1705–1712. doi:10.1016/j.physa.2007.11.004 (Mar. 1, 2008).

56. Moody, J. & Mucha, P. J. Portrait of Political Party Polarization. *Network Science* **1,** 119–121. doi:10.1017/nws.2012.3 (Apr. 2013).

57. Waugh, A. S., Pei, L., Fowler, J. H., Mucha, P. J. & Porter, M. A. *Party Polarization in Congress: A Network Science Approach* preprint.

58. Neal, Z. The Backbone of Bipartite Projections: Inferring Relationships from Co-Authorship, Co-Sponsorship, Co-Attendance and Other Co-Behaviors. *Social Networks* **39,** 84–97. doi:10.1016/j.socnet.2014.06.001 (Oct. 1, 2014).

59. Aref, S. & Wilson, M. C. Measuring Partial Balance in Signed Networks. *Journal of Complex Networks.* doi:10.1093/comnet/cnx044 (Sept. 14, 2015).

60. Cartwright, D. & Harary, F. Structural Balance: A Generalization of Heider's Theory. *Psychological Review* **63,** 277–293. doi:10.1037/h0046049 (1956).

61. Heider, F. Social Perception and Phenomenal Causality. *Psychological Review* **51,** 358–374. doi:10.1037/h0055425 (Nov. 1944).

62. Aref, S. & Wilson, M. C. Balance and Frustration in Signed Networks. *Journal of Complex Networks.* doi:10.1093/comnet/cny015 (Dec. 13, 2017).

63. *Open Data API* https://www.camara.cl/transparencia/datosAbiertos.aspx.

64. Belaza, A. M. *et al.* Statistical Physics of Balance Theory. *PLOS ONE* **12,** e0183696. doi:10.1371/journal.pone.0183696 (Aug. 28, 2017).